

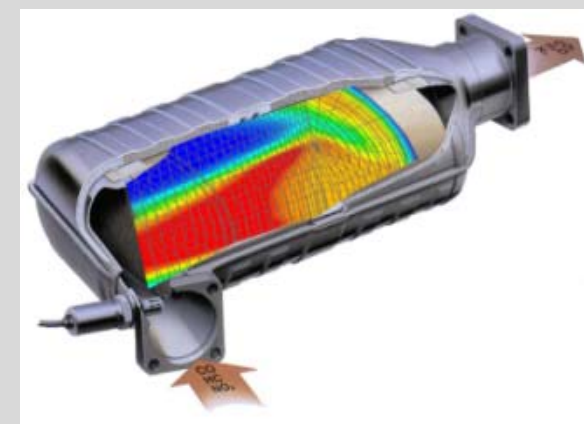
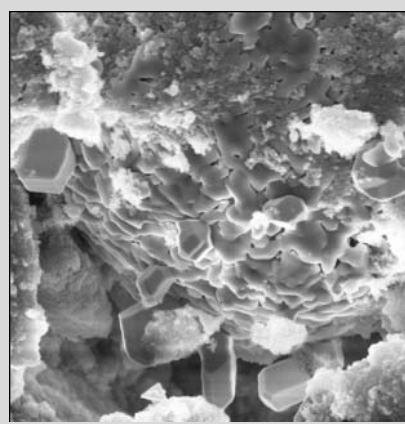
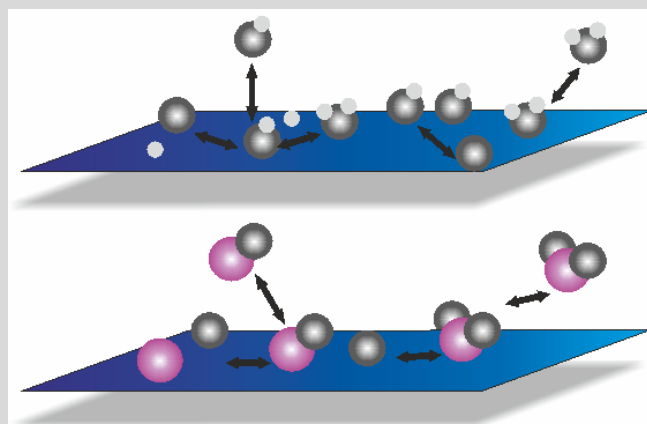
Microkinetic models for exhaust-gas after-treatment

Olaf Deutschmann, Karlsruhe Institute of Technology (KIT)

CLEERS 2015

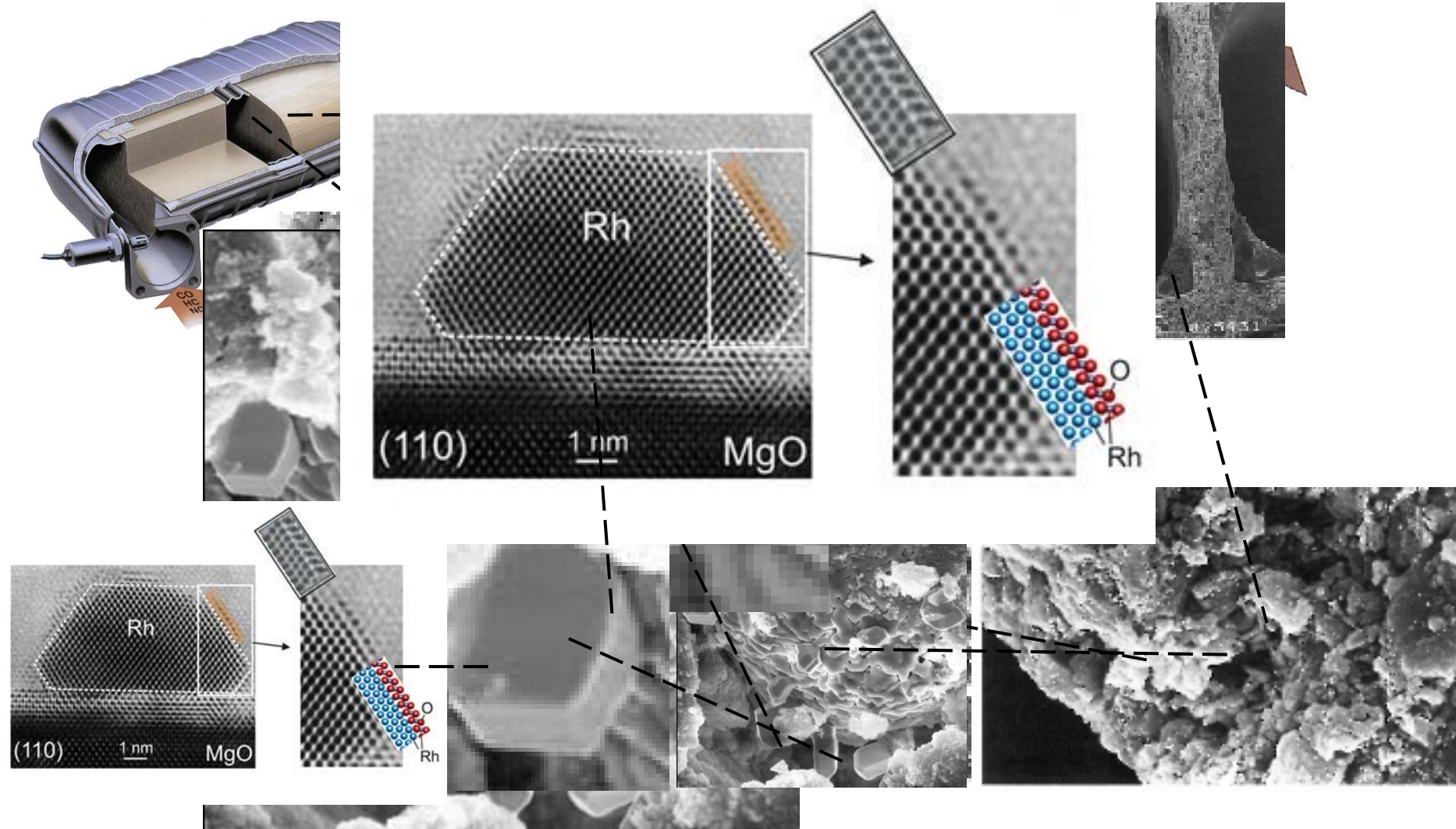
Institute for Chemical Technology and Polymer Chemistry (ITCP)

Institute for Catalysis Research and Technology (IKFT)

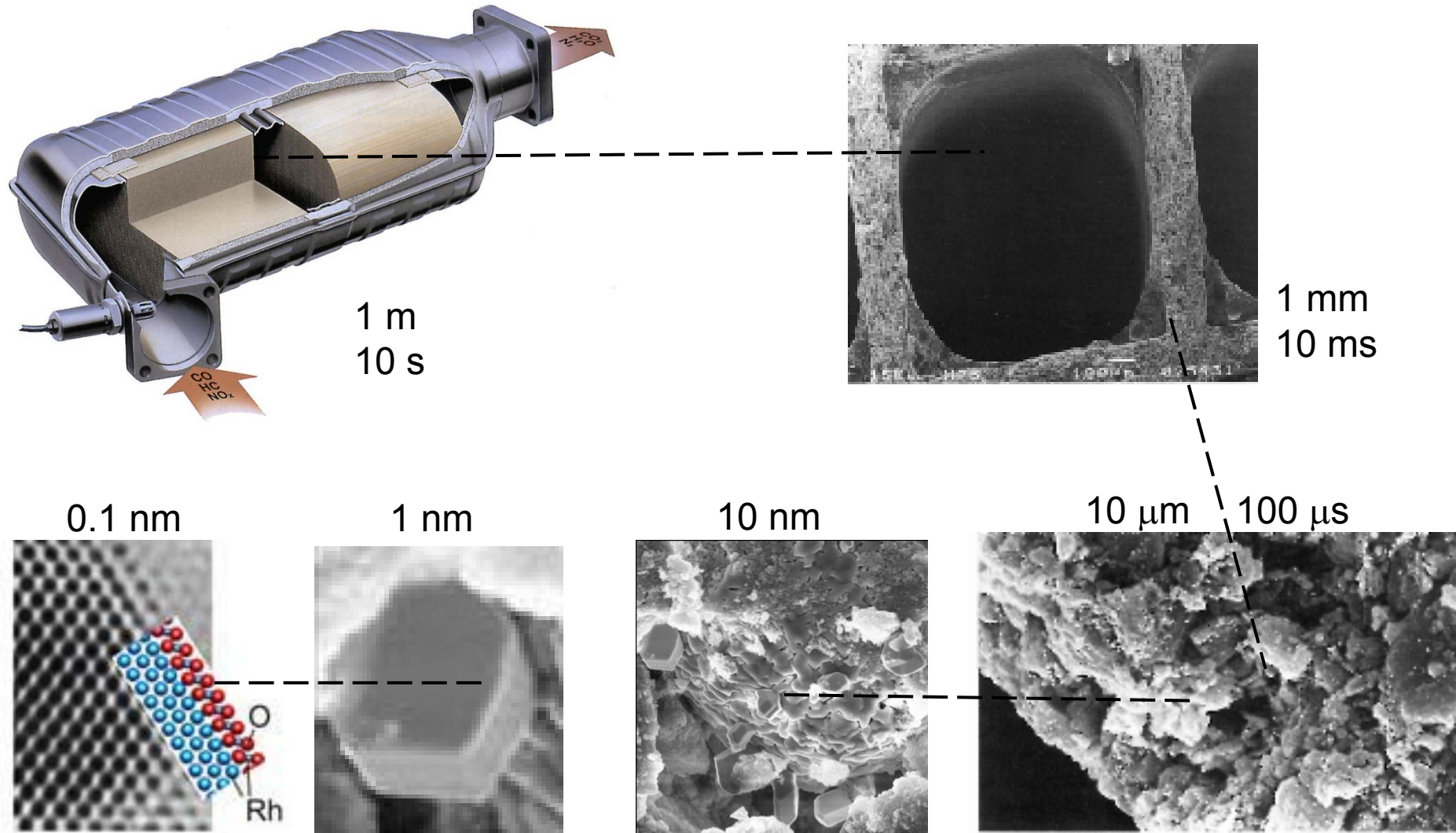


THE CHALLENGE

Catalytic converter: Physics and chemistry on many scales

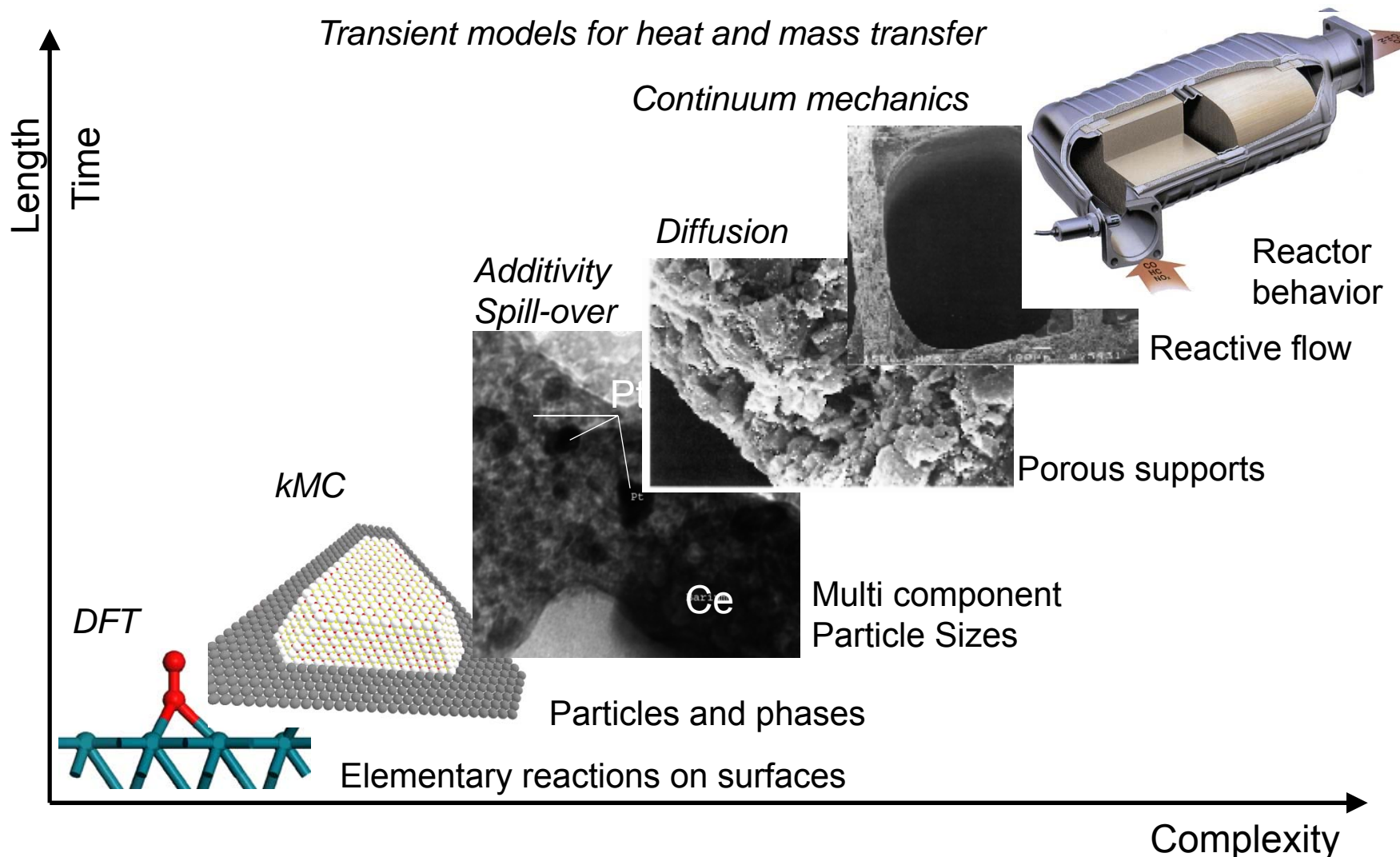


Catalytic converter: Physics and chemistry on many scales



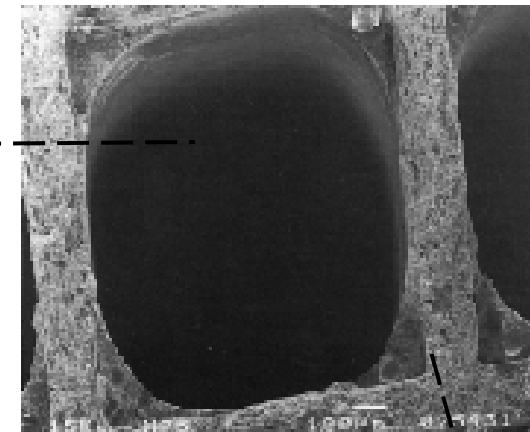
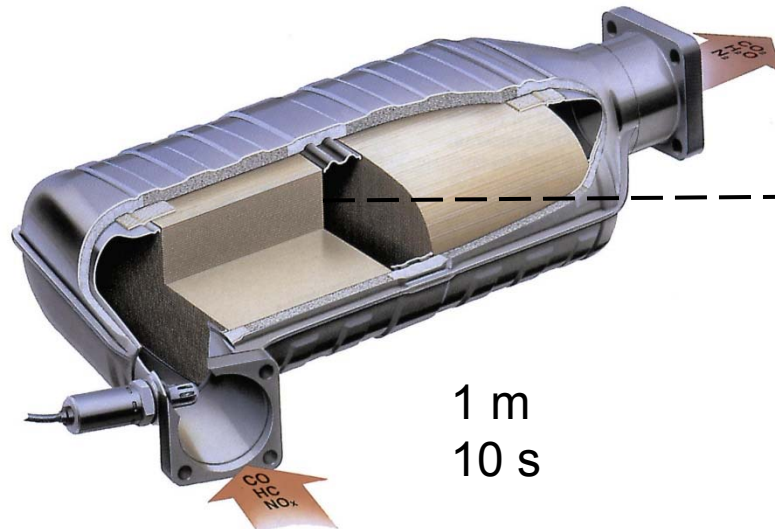
THE DREAM

Simulation of catalytic reactors by multi-scale modeling: Information flux over the time and length scales

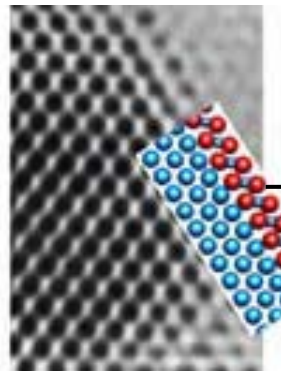


THE REALITY

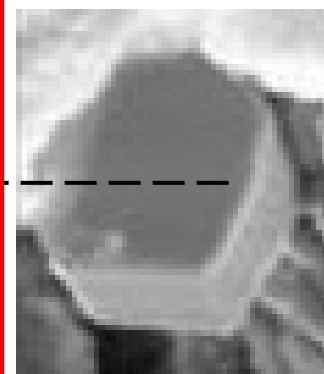
Catalytic converter: Physics and chemistry on many scales



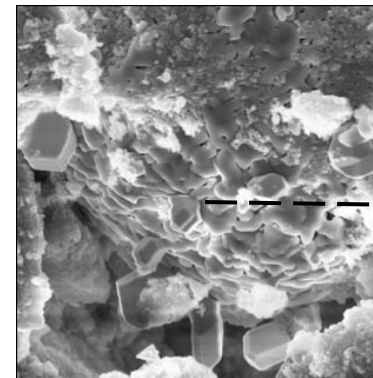
0.1 nm



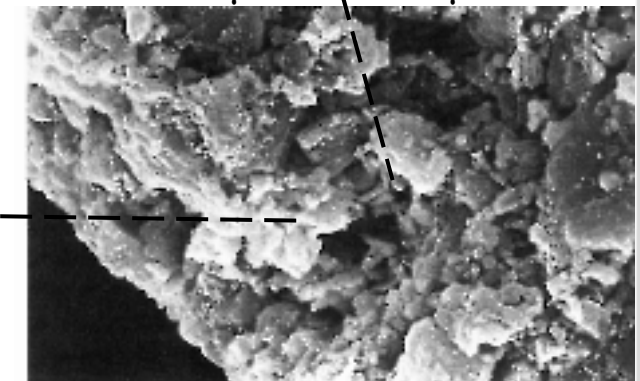
1 nm



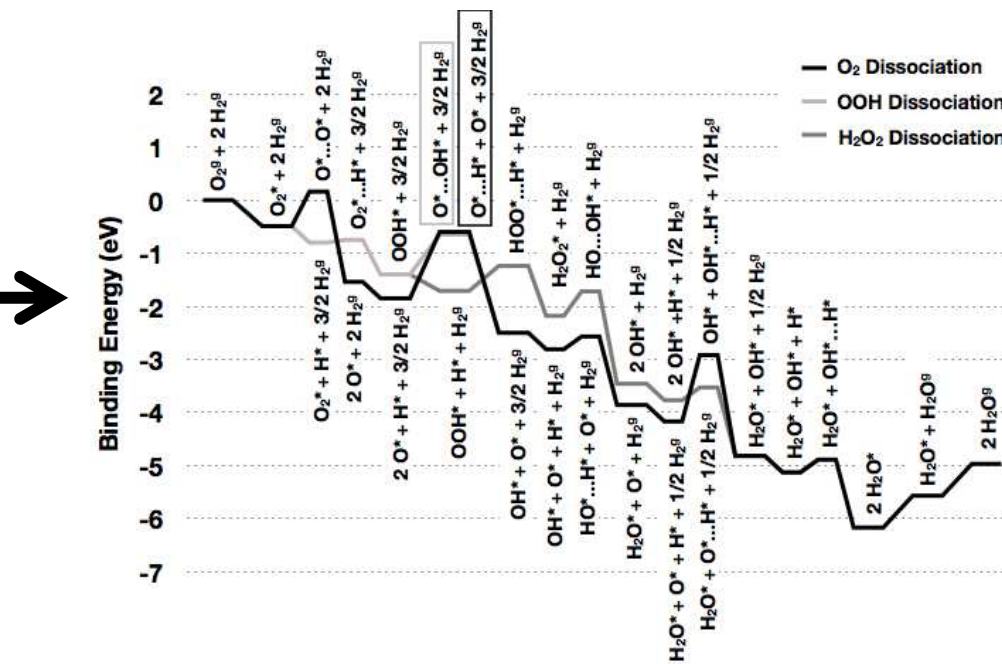
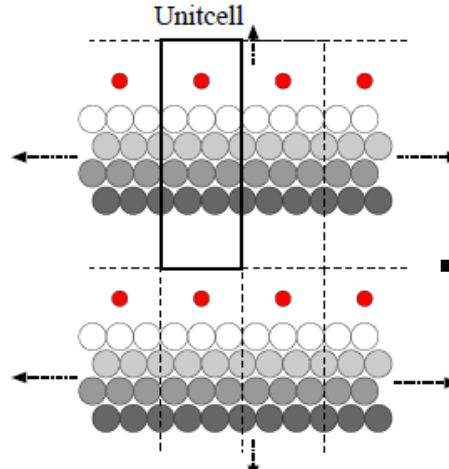
10 nm



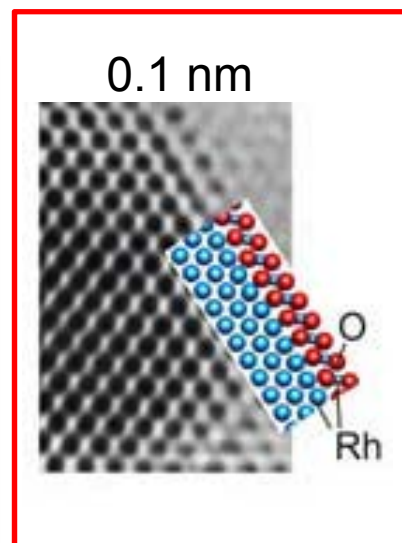
10 μ m 100 μ s



Density Functional Theory (DFT): Understanding catalysis on a molecular level

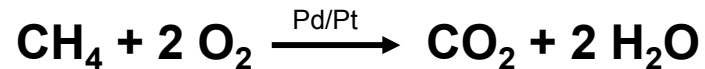


J.A. Keith, J. Anton, T.Jacob. Chapter 1 in *Modeling and Simulation of Heterogeneous Catalytic Reactions*. O. Deutschmann (Ed.), 2011

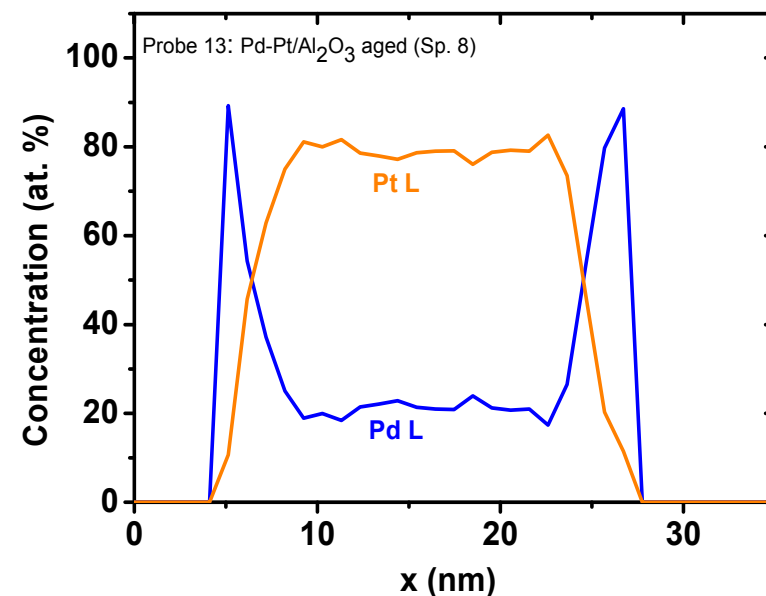
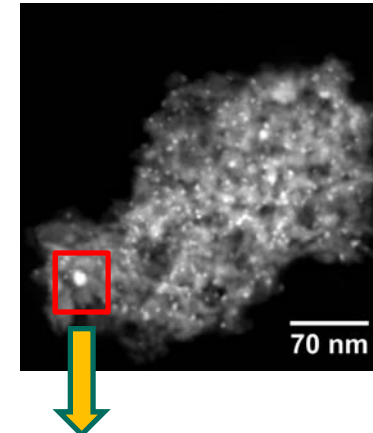


- **Energy barriers**
- **Understanding reaction paths**
- **Pre-screening of catalysts**

Aging of Pd/Pt catalyst for CH₄ total oxidation: Characterization by TEM and EDX

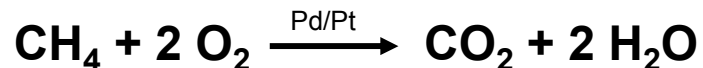


- Total Pd/Pt loading 5:1
- Most particles d < 5 nm
 - Homogenous alloy
(Pd₁₀₀Pt₀ - Pd_{89±5}Pt_{11±2})
- Some particles d ≈ 10 nm
 - Homogenous Alloy, higher Pt-content
- Few large particles d > 30 nm
 - Homogenous alloy
 - High Pt content
 - Formation of core-shell structure after 100 h, 1000 ppm CH₄, 10% O₂

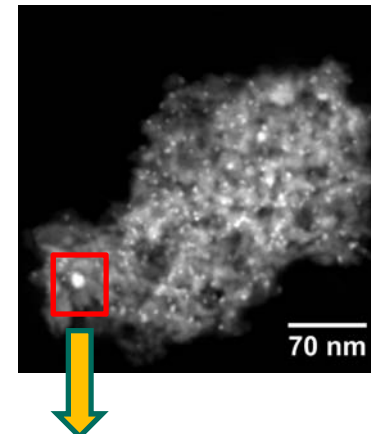


A. T. Gremminger, H. W. Pereira de Carvalho, R. Popescu, J.-D. Grunwaldt, O. Deutschmann. *Catalysis Today* (2015) DOI 10.1016/j.cattod.2015.01.034

Aging of Pd/Pt catalyst for CH₄ total oxidation: Characterization by TEM and EDX



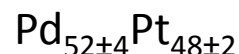
- **Total Pd/Pt loading 5:1**
- **Most particles d < 5 nm**
 - Homogenous alloy
(Pd₁₀₀Pt₀ - Pd_{89±5}Pt_{11±2})
- **Some particles d ≈ 10 nm**
 - Homogenous Alloy, higher Pt-content
- **Few large particles d > 30 nm**
 - Homogenous alloy
 - High Pt content
 - Formation of core-shell structure after 100 h, 1000 ppm CH₄, 10% O₂



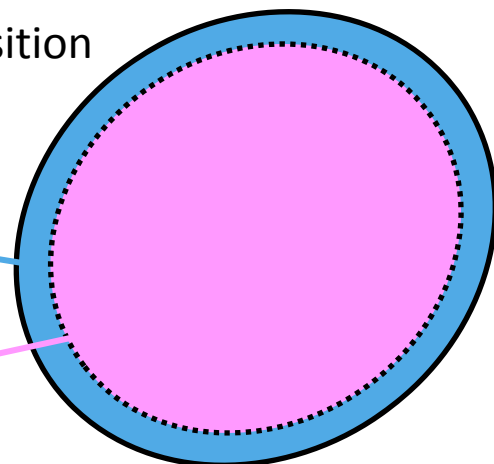
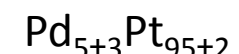
- Total NP composition



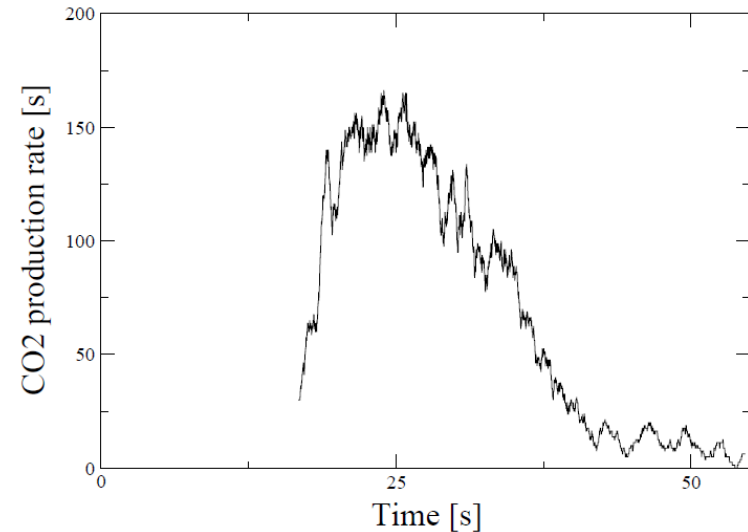
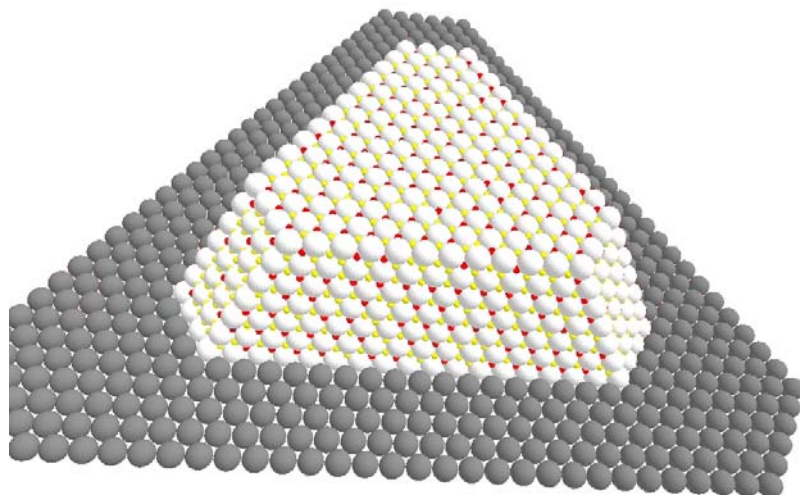
~ 3 nm shell



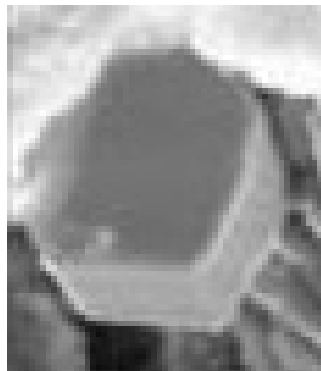
~ 22 nm core



Kinetic Monte Carlo Simulation of surface reactions and diffusion on catalytic particles: CO oxidation on Pt/Al₂O₃



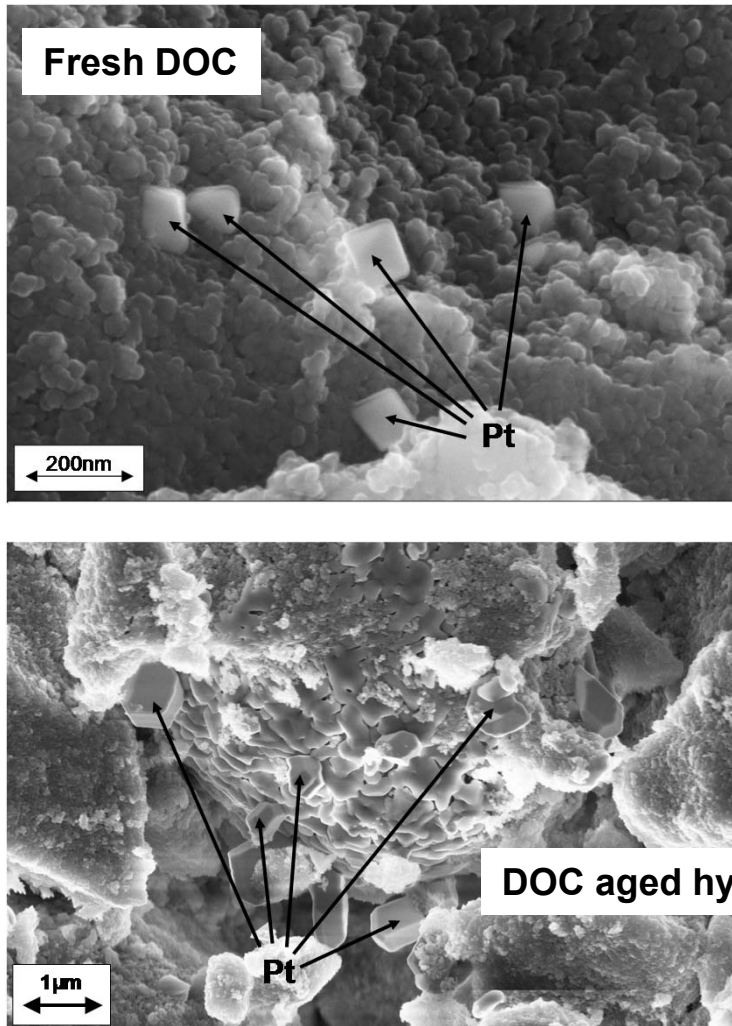
1-100 nm



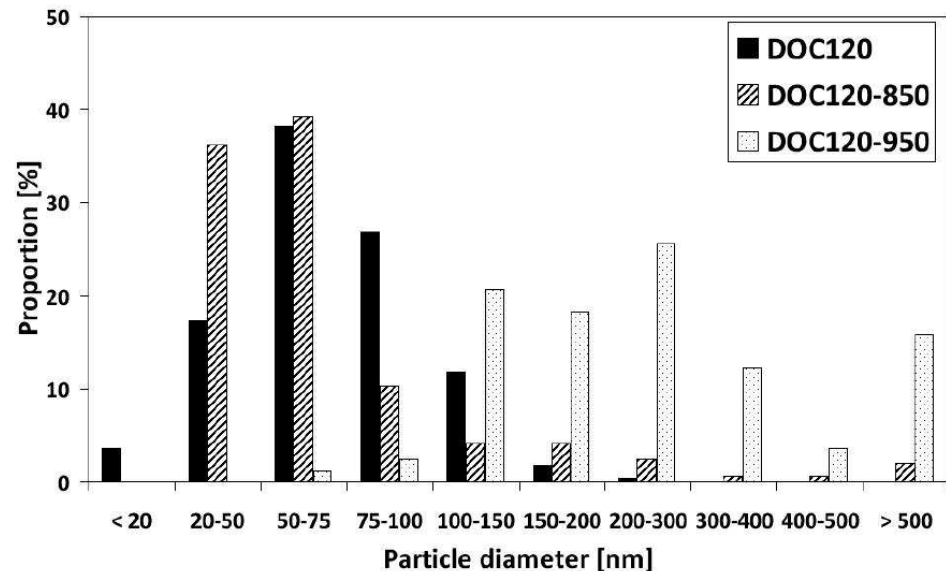
- **Coverage over time on each facet**
- **Reaction rates of each process**
- **Number of times each process was used**

L. Kunz et al., Chapter 4 in *Modeling Heterogeneous Catalytic Reactions*. O. Deutschmann (Ed.), 2011

Effect of thermal aging on particle size distribution in DOC

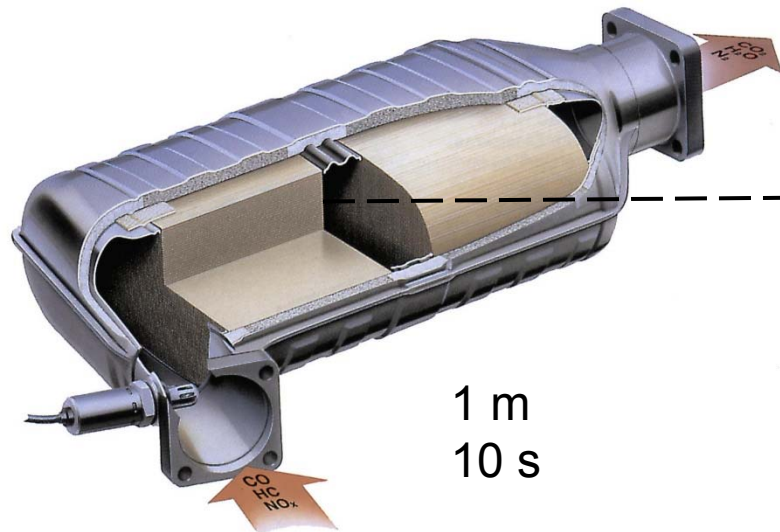


Particle size distribution

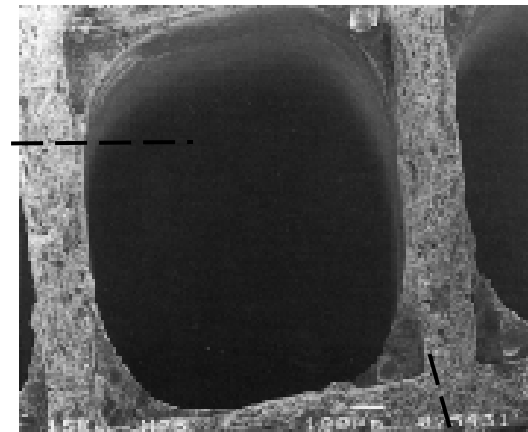


W. Boll, S. Tischer, O. Deutschmann, Ind. & Eng. Chem. Res. 49 (2010) 10303

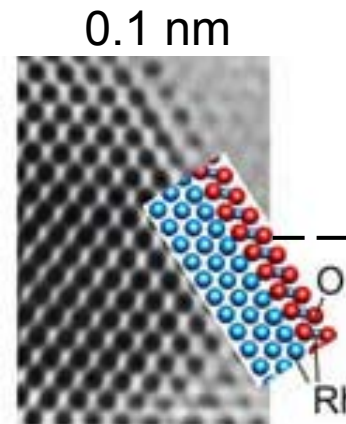
Catalytic converter: Physics and chemistry on many scales



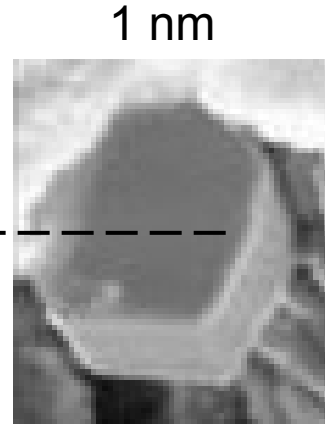
1 m
10 s



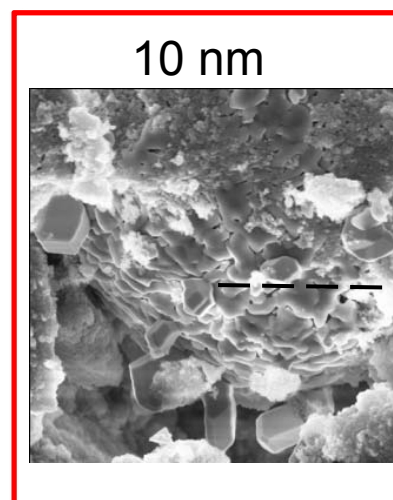
1 mm
10 ms



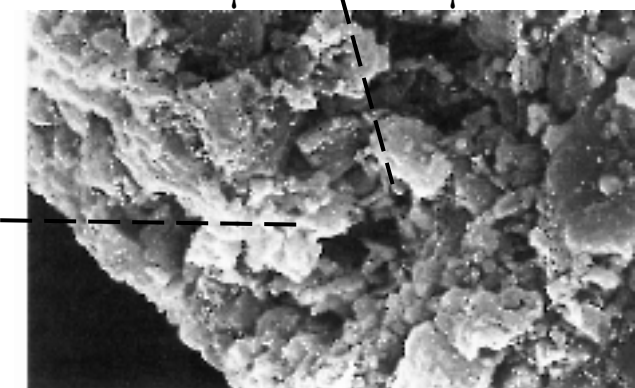
0.1 nm



1 nm

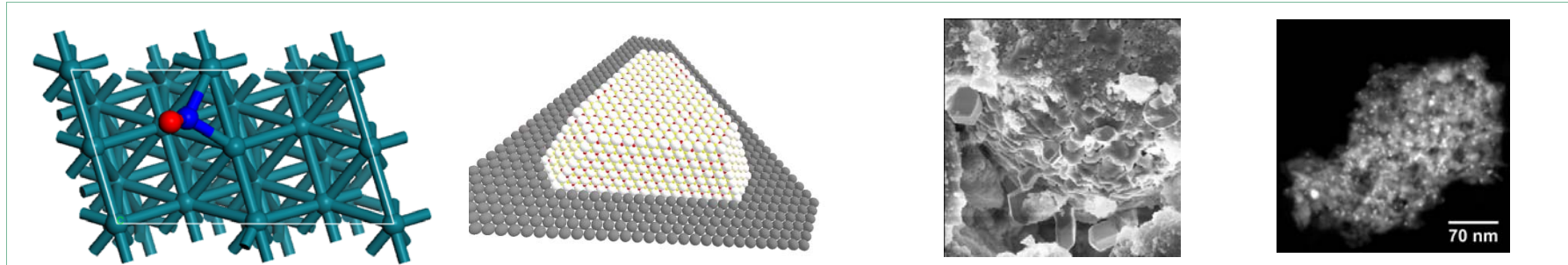


10 nm



10 μm 100 μs

Modeling heterogeneous reactions: Concept of rate equations (mean-field approximation)



Surface coverage

$$\Theta_i = \frac{c_i \sigma_i}{\Gamma} \quad \frac{\partial \Theta_i}{\partial t} = \frac{\dot{s}_i M_i}{\Gamma}$$

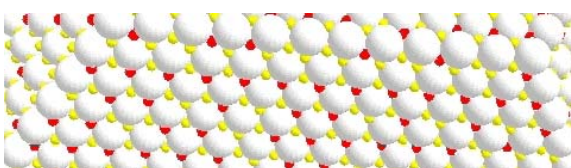
Surface reaction rate

$$\dot{s}_i = \sum_{k \in R} \nu_{ik} k_{f_k} \prod_{j \in S} c_j^{\nu'_{jk}}$$

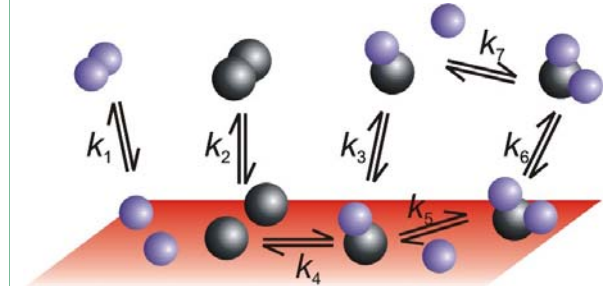
Rate expression

$$k_{f_k} = A_k T^{\beta_k} \exp\left[\frac{-E_{a_k}}{RT}\right] \prod_{i=1}^{N_s} \Theta_i^{\mu_{i_k}} \exp\left[\frac{\varepsilon_{i_k} \Theta_i}{RT}\right]$$

Γ = microscopic site density

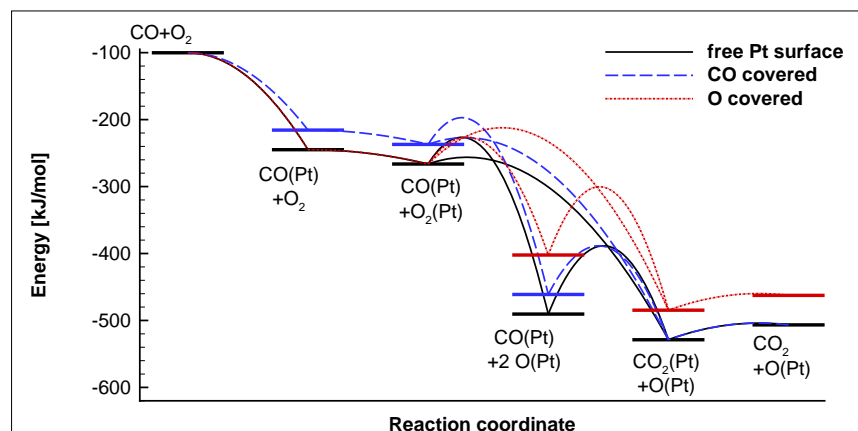
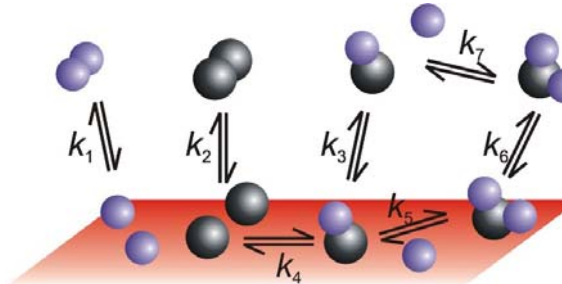
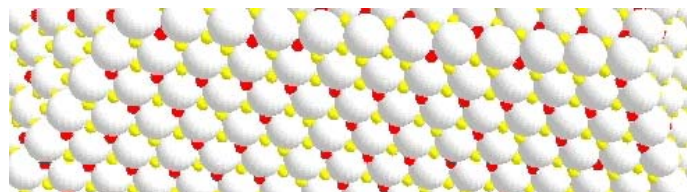


Locally resolved reaction rates depending on gas-phase concentration and surface coverages



O. Deutschmann. in *Handbook of Heterogeneous Catalysis*, 2nd Ed., G. Ertl, H. Knözinger, F. Schüth, J. Weitkamp (eds.), p. 1811, Wiley-VCH, 2008

Surface reaction kinetics of CO oxidation on Pt/Al₂O₃ DOC: Mean field approximation



Reaction	A [mol, cm, s] / S^0	β	E_a [kJ/mol]
$O_2 + (Pt) \rightarrow O_2(Pt)$	5.000×10^{-2}	0.000	0.00
$O_2(Pt) \rightarrow O_2 + (Pt)$	5.243×10^{11}	-0.069	19.573
$O_2(Pt) + (Pt) \rightarrow O(Pt) + O(Pt)$	8.325×10^{18}	0.000	39.933
$O(Pt) + O(Pt) \rightarrow O_2(Pt) + (Pt)$	4.444×10^{21}	0.000	264.067
			$-88.2 \times \Theta_O$
$CO + (Pt) \rightarrow CO(Pt)$	8.400×10^{-1}	0.000	0.000
$CO(Pt) \rightarrow CO + (Pt)$	7.635×10^{12}	-0.139	143.145
			$-29.3 \times \Theta_{CO}$
$CO_2 + (Pt) \rightarrow CO_2(Pt)$	3.193×10^{-3}	-0.035	2.686
$CO_2(Pt) \rightarrow CO_2 + (Pt)$	1.894×10^{10}	0.139	21.855
$CO(Pt) + O_2(Pt) \rightarrow CO_2(Pt) + O(Pt)$	4.124×10^{18}	0.069	9.494
			$+44.1 \times \Theta_O$
$CO_2(Pt) + O(Pt) \rightarrow CO(Pt) + O_2(Pt)$	2.910×10^{23}	-0.069	272.506
			$+29.3 \times \Theta_{CO}$
$CO(Pt) + O(Pt) \rightarrow CO_2(Pt) + (Pt)$	4.764×10^{18}	0.069	101.361
			$-29.3 \times \Theta_{CO}$
$CO_2(Pt) + (Pt) \rightarrow CO(Pt) + O(Pt)$	6.297×10^{20}	-0.069	140.239
			$+44.1 \times \Theta_O$

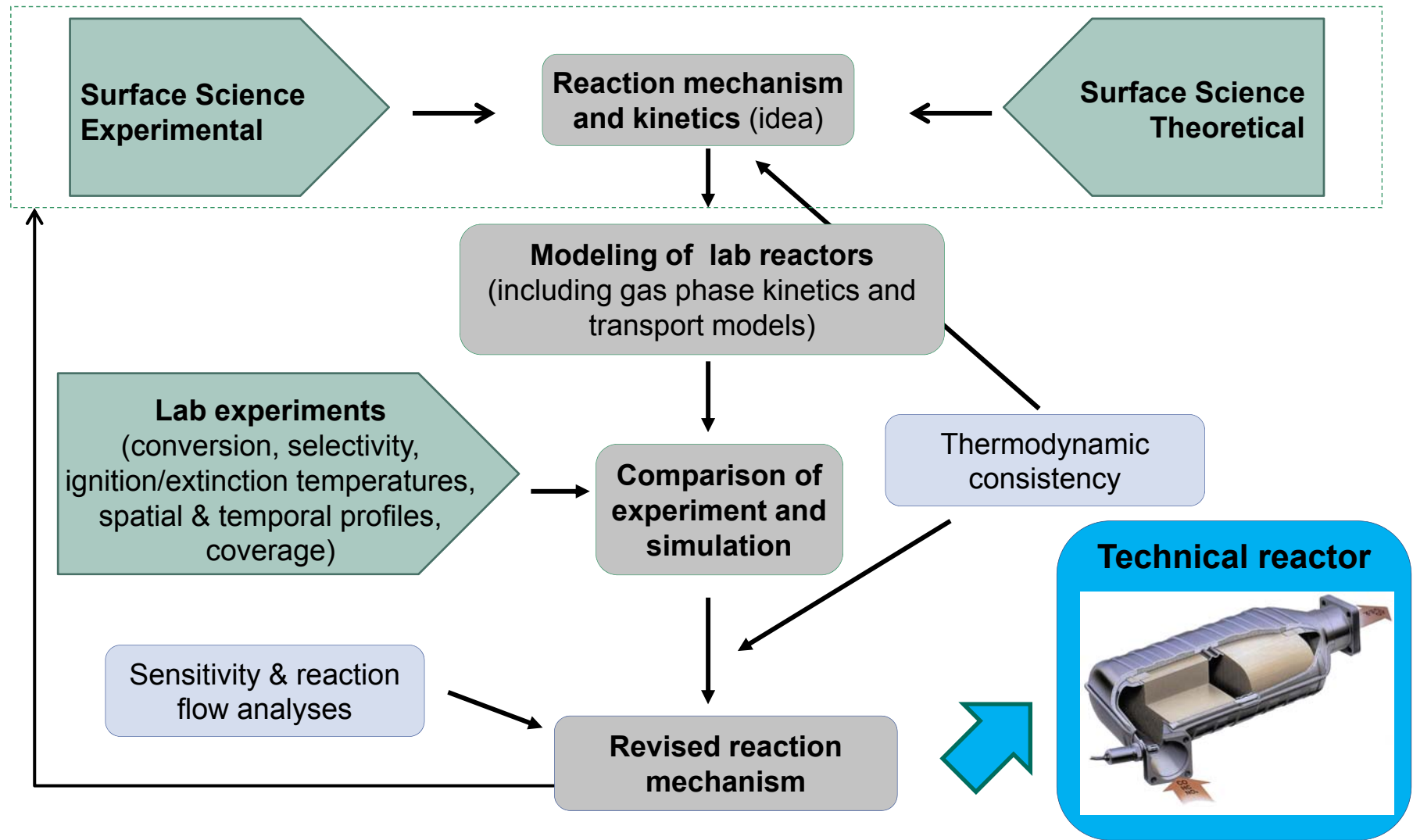
D. Chan, S. Tischer, J. Heck, C. Diehm, O. Deutschmann. Applied Catalysis B: Environmental 156–157 (2014) 153.

Proposed surface reaction mechanism for Pt/Rh-based three-way catalysts: Mean field approximation

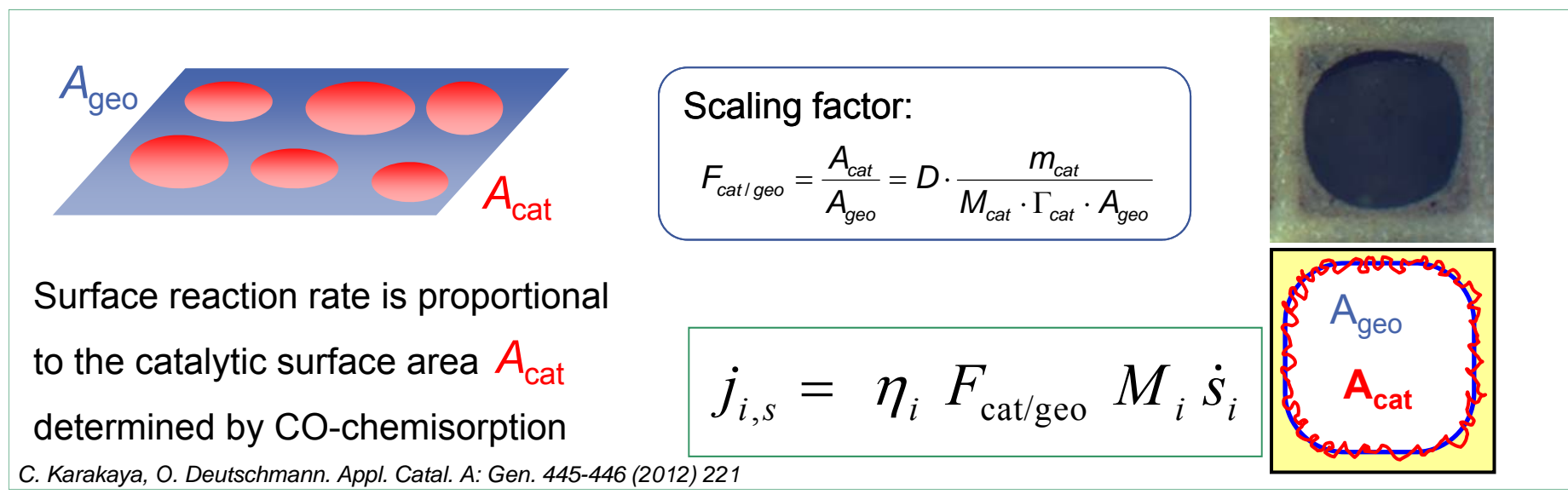
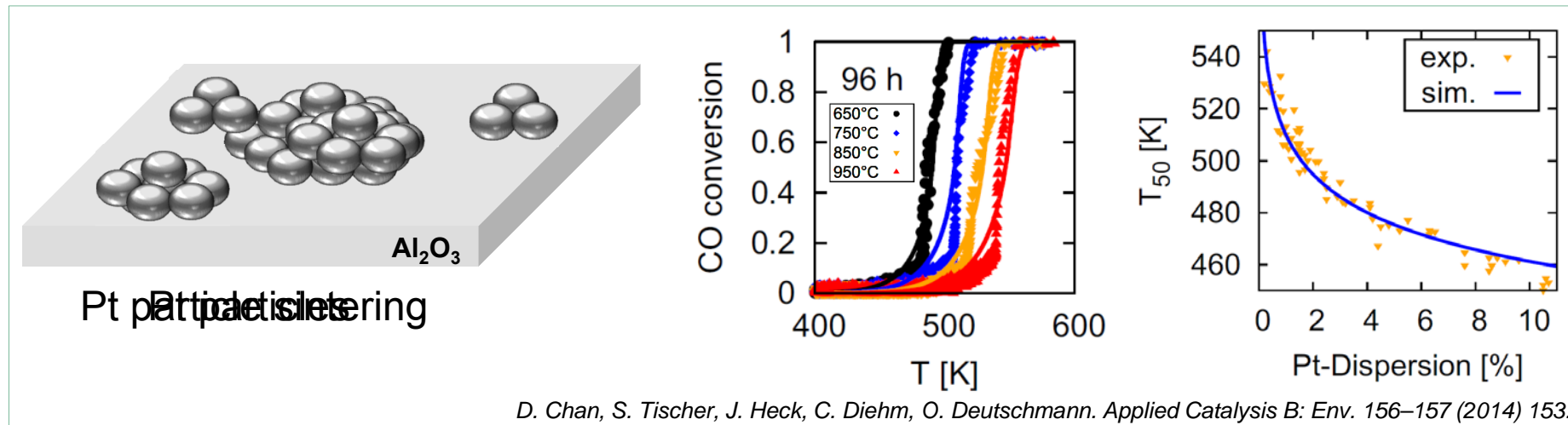
	A (mole, cm, s)	E_a (kJ/mol)								
Adsorption/desorption reactions										
$C_3H_6(s) + Pt(s) + Pt(s) \rightarrow C_3H_6(s)$	$S^0 = 0.98$		$C_2H_3(s) + O(s) \rightarrow CH_3CO(s) + Pt(s)$	3.7×10^{19}	62.3					
$C_3H_6(s) \rightarrow Pt(s) + Pt(s) + C_3H_6$	3.7×10^{12}	74.4	$CH_3CO(s) + Pt(s) \rightarrow C_2H_3(s) + O(s)$	7.9×10^{20}	191.4	$+60\Theta_{O(s)}$				
$C_3H_6(s) + O(s) \rightarrow C_3H_5(s) + OH(s)$	$S^0 = 0.05$		$CH_3(s) + CO(s) \rightarrow CH_3CO(s) + Pt(s)$	3.7×10^{21}	82.9					
$\mu(\Theta_{Pt(s)}) = -0.9$			$CH_3CO(s) + Pt(s) \rightarrow CH_3(s) + CO(s)$	1.8×10^{23}	6.1	$+33\Theta_{CO(s)}$				
$C_3H_5(s) + OH(s) \rightarrow O(s) + Pt(s) + C_3H_6$	3.7×10^{21}	31.0	$CH_3(s) + O(s) \rightarrow OH(s) + CH_2(s)$	3.7×10^{21}	36.6					
$CH_4 + Pt(s) + Pt(s) \rightarrow CH_3(s) + H(s)$	$S^0 = 0.01$		$OH(s) + CH_2(s) \rightarrow CH_3(s) + O(s)$	2.3×10^{22}	26.0					
$O_2 + Pt(s) + Pt(s) \rightarrow O(s) + O(s)$	$S^0 = 0.07$		$CH_2(s) + O(s) \rightarrow OH(s) + CH(s)$	3.7×10^{21}	25.1					
$O(s) + O(s) \rightarrow Pt(s) + Pt(s) + O_2$	3.2×10^{21}	224.7	$OH(s) + CH(s) \rightarrow CH_2(s) + O(s)$	1.2×10^{21}	26.8					
			$CH(s) + O(s) \rightarrow OH(s) + C(s)$	3.7×10^{21}	25.1					
			$OH(s) + C(s) \rightarrow CH(s) + O(s)$	1.9×10^{21}	214.2					
$H_2 + Pt(s) + Pt(s) \rightarrow H(s) + H(s)$	$S^0 = 0.046$									
$H(s) + H(s) \rightarrow Pt(s) + Pt(s) + H_2$	2.1×10^{21}	69.1								
$H_2O + Pt(s) \rightarrow H_2O(s)$	$S^0 = 0.75$									
$H_2O(s) \rightarrow Pt(s) + H_2O$	5.0×10^{13}	49.2								
$CO_2 + Pt(s) \rightarrow CO_2(s)$	$S^0 = 0.005$									
$CO_2(s) \rightarrow Pt(s) + CO_2$	3.6×10^{10}	23.7								
$CO + Pt(s) \rightarrow CO(s)$	$S^0 = 0.84$									
$CO(s) \rightarrow Pt(s) + CO$	2.1×10^{13}	136.2								
$NO + Pt(s) \rightarrow NO(s)$	$S^0 = 0.85$									
$NO(s) \rightarrow Pt(s) + NO$	2.1×10^{12}	80.7								
$NO_2 + Pt(s) \rightarrow NO_2(s)$	$S^0 = 0.9$									
$NO_2(s) \rightarrow Pt(s) + NO_2$	1.4×10^{13}	61.0								
$N_2O + Pt(s) \rightarrow N_2O(s)$	$S^0 = 0.025$									
$N_2O(s) \rightarrow Pt(s) + N_2O$	1.2×10^{10}	0.7								
$N(s) + N(s) \rightarrow Pt(s) + Pt(s) + N_2$	3.7×10^{21}	113.9								
Surface reactions										
Propylene oxidation										
$C_3H_6(s) \rightarrow C_3H_5(s) + H(s)$	1.0×10^{13}	75.4								
$C_3H_5(s) + H(s) \rightarrow C_3H_6(s)$	3.7×10^{21}	48.8								
$C_3H_5(s) + Pt(s) \rightarrow C_2H_3(s) + CH_2(s)$	3.7×10^{21}	108.2								
$C_2H_3(s) + CH_2(s) \rightarrow C_3H_5(s) + Pt(s)$	3.7×10^{21}	3.3								
$C_2H_3(s) + Pt(s) \rightarrow CH_3(s) + C(s)$	3.7×10^{21}	46.0								
$CH_3(s) + C(s) \rightarrow C_2H_3(s) + Pt(s)$	3.7×10^{21}	46.5								
$CH_3(s) + Pt(s) \rightarrow CH_2(s) + H(s)$	1.3×10^{22}	70.4								
$CH_2(s) + H(s) \rightarrow CH_3(s) + Pt(s)$	2.9×10^{22}	0.4								
$CH_2(s) + Pt(s) \rightarrow CH(s) + H(s)$	7.0×10^{22}	59.2								
$CH(s) + H(s) \rightarrow CH_2(s) + Pt(s)$	8.1×10^{21}	0.7								
$CH(s) + Pt(s) \rightarrow C(s) + H(s)$	3.1×10^{22}	0.0								
$C(s) + H(s) \rightarrow CH(s) + Pt(s)$	5.8×10^{21}	128.9								
$C_3H_5(s) + O(s) \rightarrow C_3H_4(s) + OH(s)$	5.0×10^{21}	70.0								
$C_3H_4(s) + 4O(s) + 2Pt(s) \rightarrow 3C(s) + 4OH(s)$	2.6×10^{64}	0.0 ^a								
Carbon monoxide oxidation										
$CO(s) + O(s) \rightarrow CO_2(s) + Pt(s)$					3.7×10^{21}	48.2				
$OH(s) + OH(s) \rightarrow H_2O(s) + O(s)$					2.5×10^{20}	38.2				
$H_2O(s) + O(s) \rightarrow OH(s) + OH(s)$					3.7×10^{21}	94.2				
$CO(s) + OH(s) \rightarrow HCOO(s) + Pt(s)$					1.3×10^{21}	0.9				
$HCOO(s) + Pt(s) \rightarrow CO(s) + OH(s)$					3.7×10^{21}	0.0				
$HCOO(s) + O(s) \rightarrow OH(s) + CO_2(s)$					2.8×10^{21}	151.1				
$OH(s) + CO_2(s) \rightarrow HCOO(s) + O(s)$					3.7×10^{21}	0.0				
$HCOO(s) + Pt(s) \rightarrow H(s) + CO_2(s)$					2.8×10^{21}	90.1				
$H(s) + CO_2(s) \rightarrow HCOO(s) + Pt(s)$										
Reactions of hydroxyl species										
$H(s) + O(s) \rightarrow OH(s) + Pt(s)$					5.0×10^{20}	107.8				
$OH(s) + Pt(s) \rightarrow H(s) + O(s)$					1.0×10^{21}	$+33\Theta_{CO(s)}$				
$N(s) + O(s) \rightarrow NO(s) + Pt(s)$					2.0×10^{13}	122.6				
$O(s) + NO \rightarrow NO_2(s)$					6.4×10^{21}	$-60\Theta_{O(s)}$				
$NO_2(s) \rightarrow O(s) + NO$					1.0×10^{21}	111.3				
$N(s) + NO(s) \rightarrow N_2O(s) + Pt(s)$					2.9×10^{24}	$+75\Theta_{CO(s)}$				
$N_2O(s) + Pt(s) \rightarrow N(s) + NO(s)$					1.3×10^{17}	$-60\Theta_{O(s)}$				
$NO_2(s) + Pt(s) \rightarrow O(s) + NO(s)$					8.1×10^{18}	115.5				
$H(s) + NO(s) \rightarrow OH(s) + N(s)$					1.2×10^{21}	90.9				
$OH(s) + N(s) \rightarrow H(s) + NO(s)$					2.9×10^{24}	133.1				
$NO_2(s) + H(s) \rightarrow OH(s) + NO(s)$					1.3×10^{17}	133.0				
$OH(s) + NO(s) \rightarrow NO_2(s) + H(s)$					6.4×10^{21}	$+75\Theta_{CO(s)}$				
$NO_2(s) + H(s) \rightarrow OH(s) + NO(s)$					3.9×10^{21}	25.0				
$OH(s) + NO(s) \rightarrow NO_2(s) + H(s)$					6.1×10^{22}	$+80\Theta_{CO(s)}$				
Reactions of NO and NO₂										
$NO(s) + Pt(s) \rightarrow N(s) + O(s)$					3.7×10^{21}	99.9				
$N(s) + O(s) \rightarrow NO(s) + Pt(s)$					3.9×10^{21}	20.0				
$NO_2(s) + Pt(s) \rightarrow O(s) + NO(s)$					6.1×10^{22}	175.3				

D. Chatterjee, O. Deutschmann, J. Warnatz. Faraday Discuss. 119 (2001) 371
 J. Koop, O. Deutschmann. Appl. Catal. B: Env. 91 (2009) 47

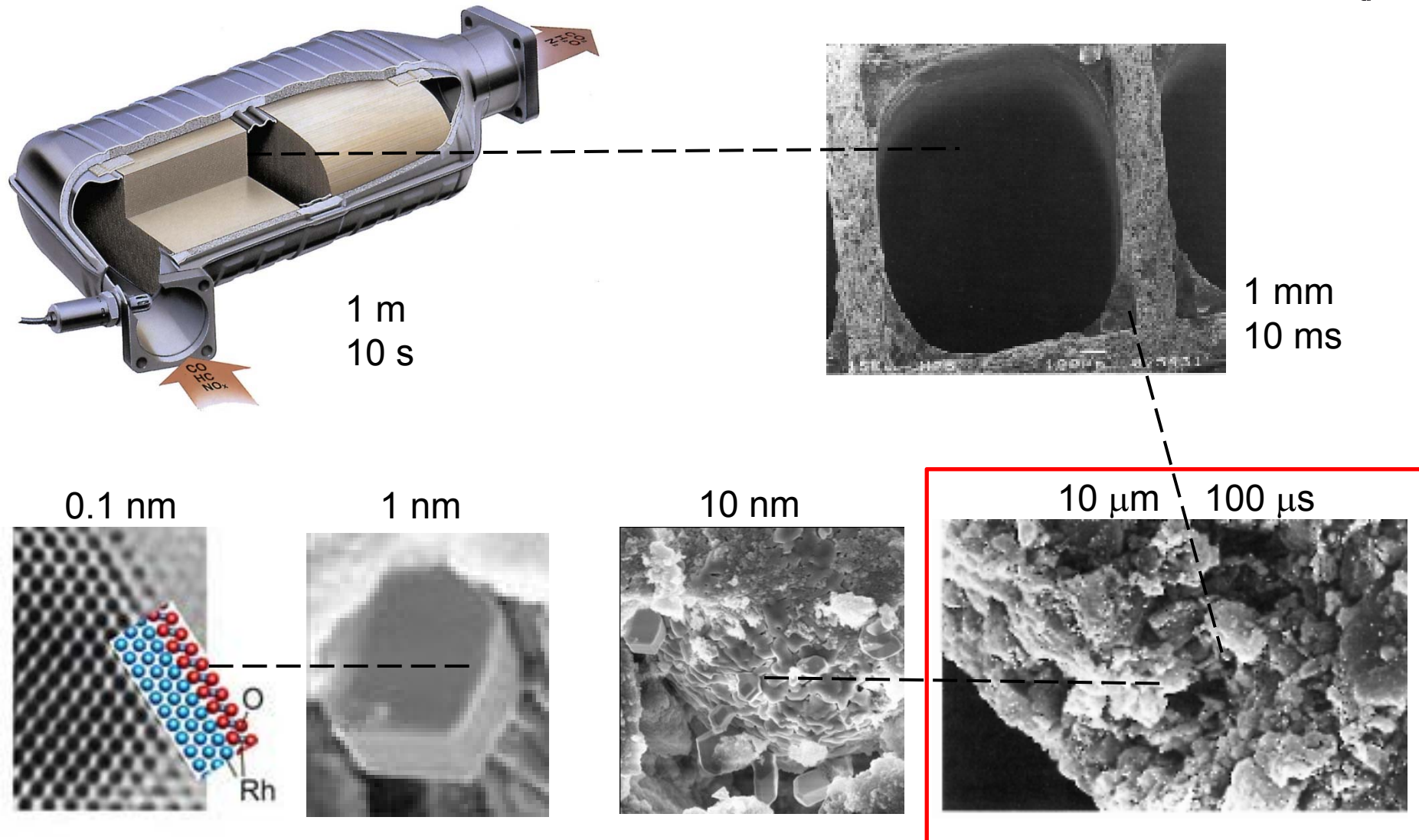
Development of micro kinetic models for simulations of catalytic reactors



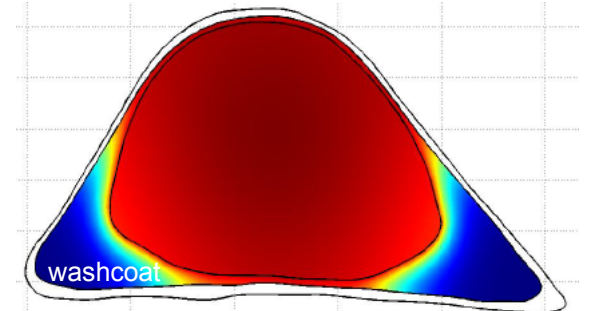
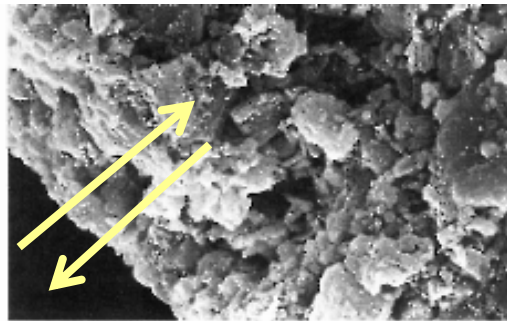
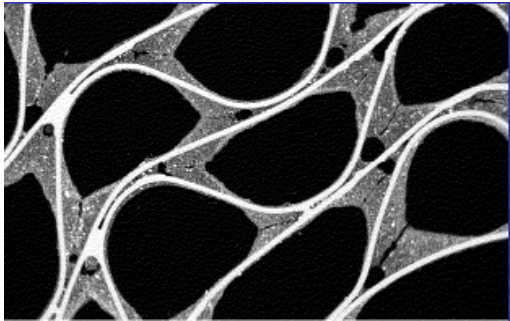
Modeling catalyst loading and dispersion: Variation of dispersion in a DOC due to aging



Multi-scale modeling: From 10^{-10} m and 10^{-13} s to 1m and 10 s



Coupling of surface reaction rate and flow field - Modeling internal transport limitation of reaction rate



R.E. Hayes, B. Liu, M. Votsmeier. Chem. Eng. Sci. 60 (2005) 2037.

Simple model: effectiveness factor

Thiele Modulus $\Phi_i = L \sqrt{\frac{\dot{s}_i \gamma}{D_{\text{eff},i} c_{i,0}}}$

Effectiveness factor $\eta_i = \frac{\tanh(\Phi_i)}{\Phi_i}$

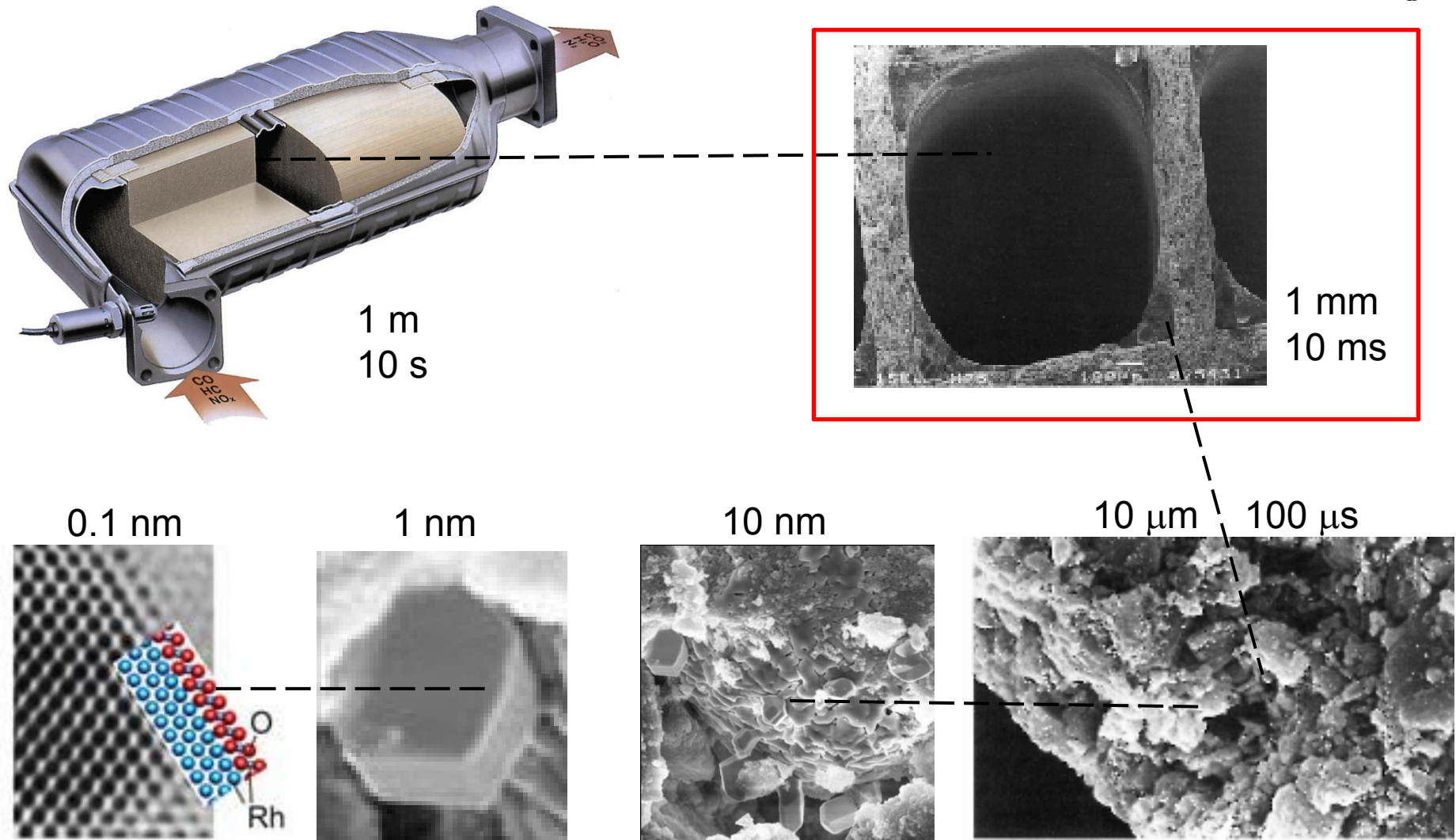
$$j_{i,s} = \eta_i F_{\text{cat/geo}} M_i \dot{s}_i$$

Reaction-diffusion equations

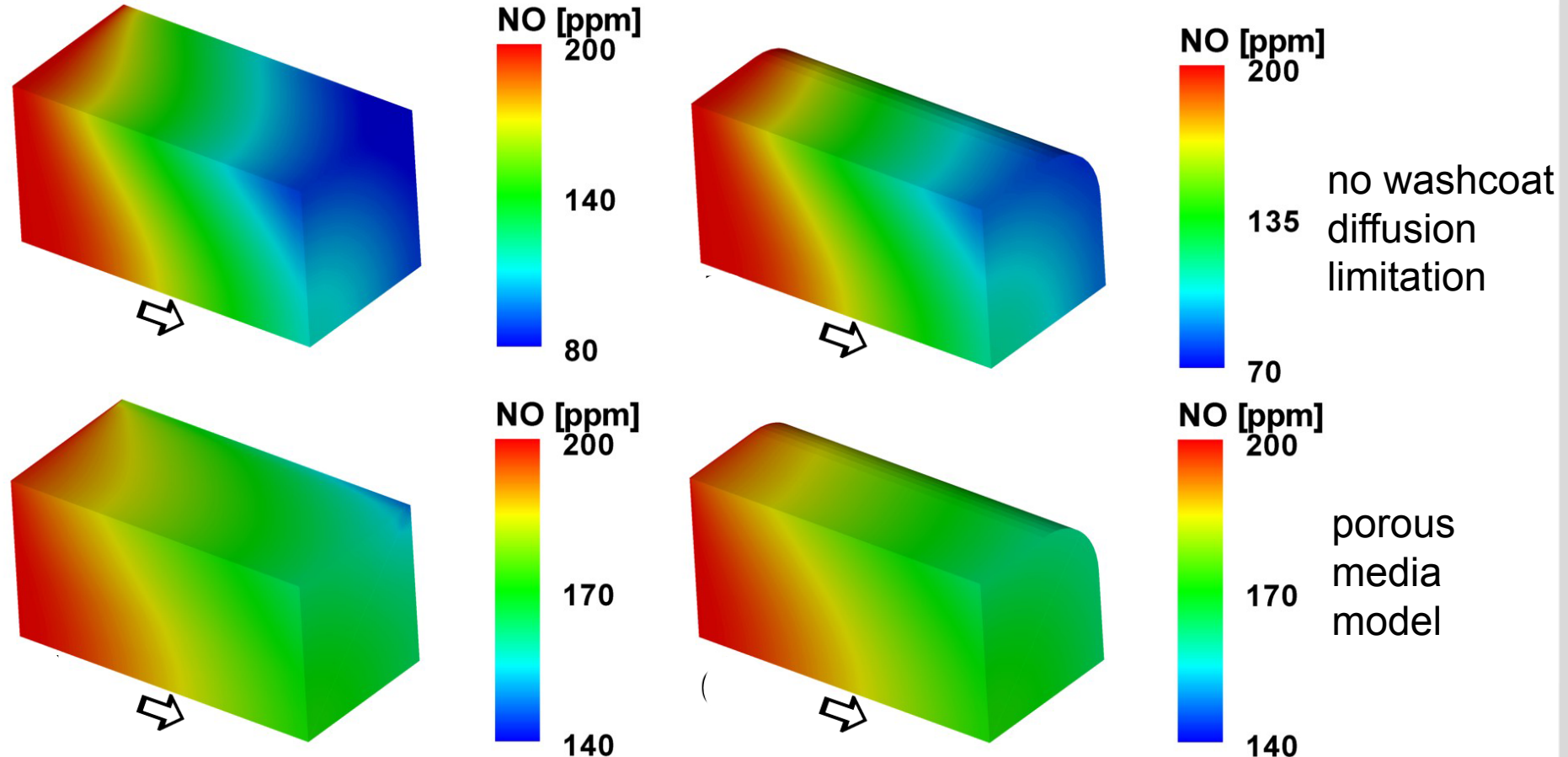
$$\nabla \cdot (D_i \nabla C_i) - \nabla \cdot (v C_i) = \frac{\partial C_i}{\partial t}$$

$$(D_{\text{eff}})_i \nabla^2 C_i - (-R_i) = \varepsilon \frac{\partial C_i}{\partial t}$$

Multi-scale modeling: From 10^{-10} m and 10^{-13} s to 1m and 10 s



Impact of models for channel shape and washcoat diffusion on NO profiles in a DOC

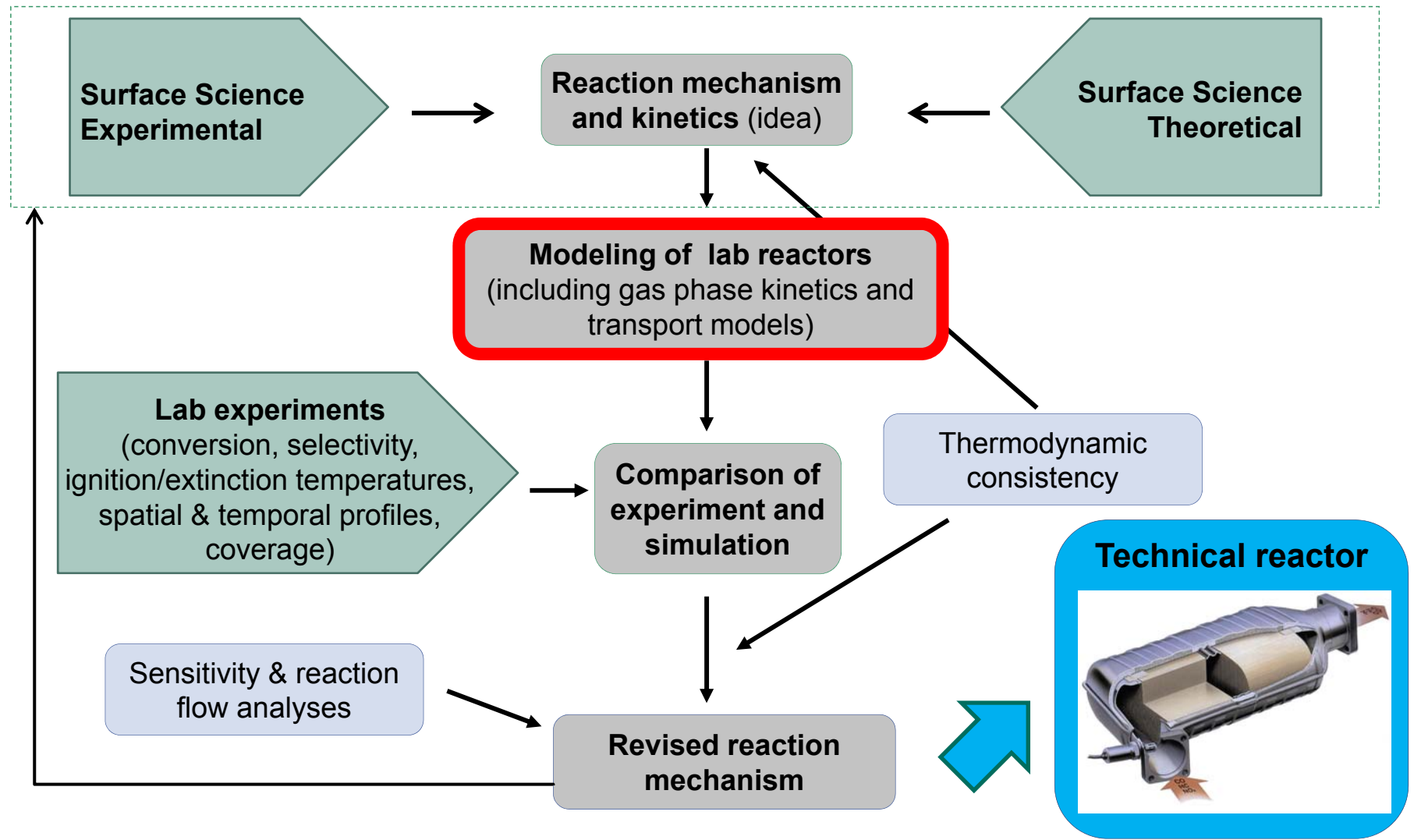


NO profiles at lean conditions at 250°C (steady-state operation)

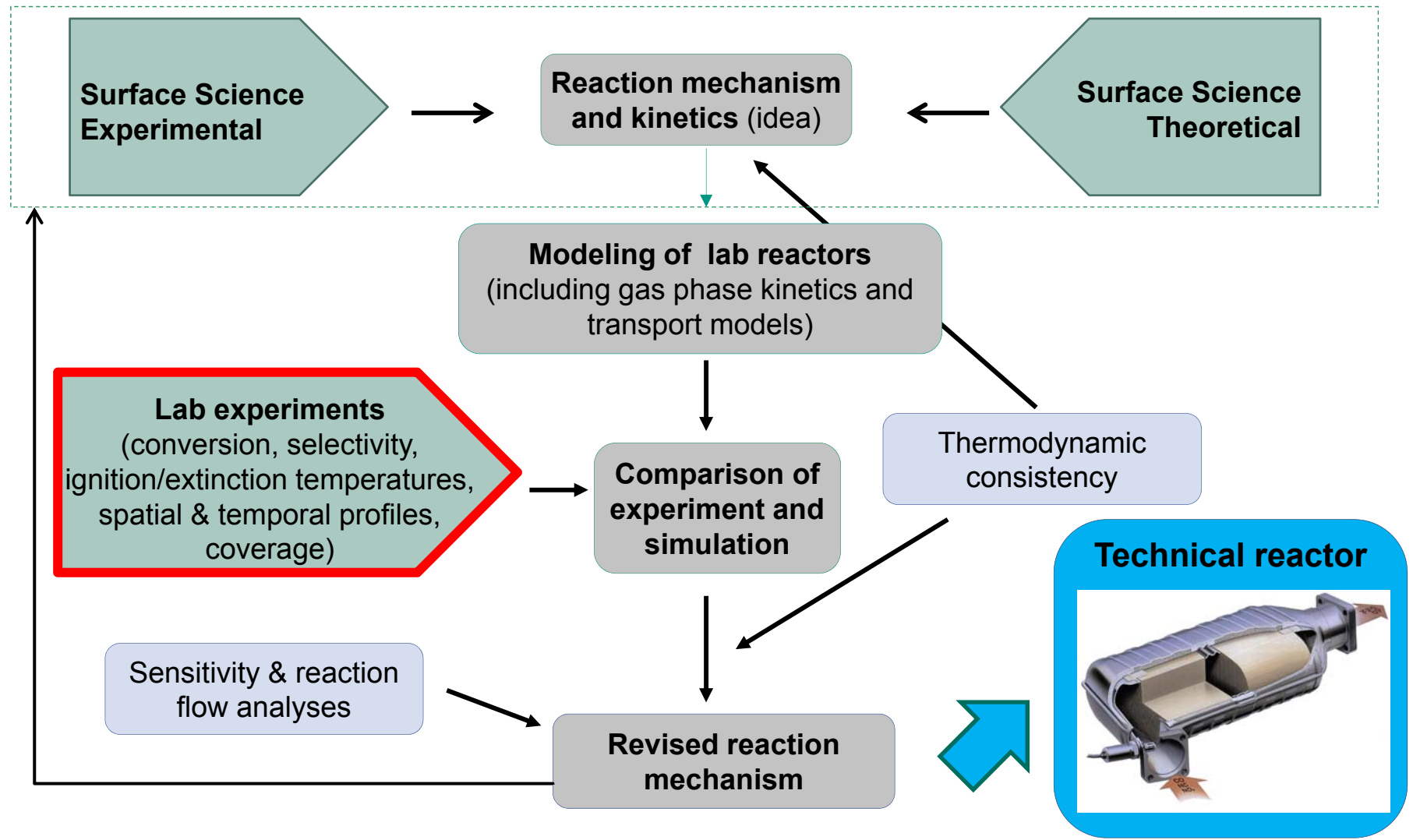
CFD code: Fluent + DETCHEM

N. Mladenov, J. Koop, S. Tischer, O. Deutschmann. Chem. Eng. Sci. 65 (2010) 812

Development of micro kinetic models for simulations of catalytic reactors



Development of micro kinetic models for simulations of catalytic reactors



Lab test benches in the Exhaust-Gas Center Karlsruhe: High-Pressure setup



Tests of catalyst coated honeycombs

($d = 2.54$ cm, length < 6cm)

Labview automatic controlled measurements

Coated pipes, reactor and analytics – for sulfur

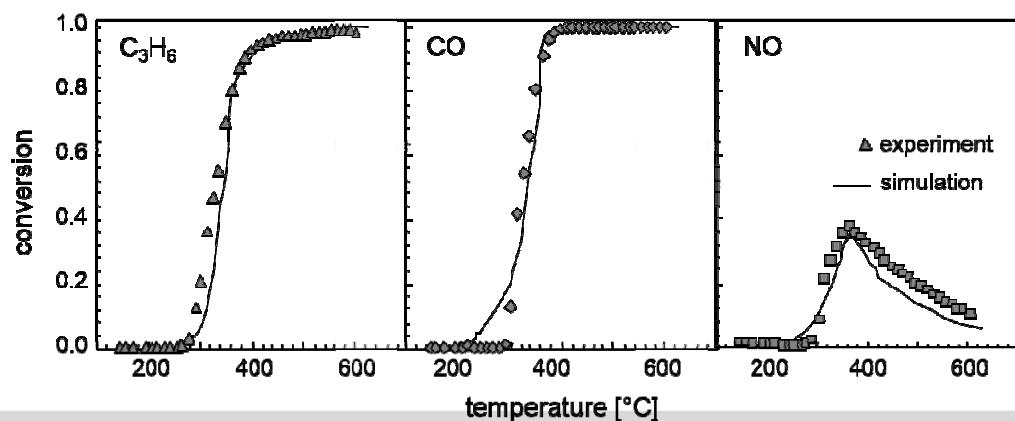
Gases: NO, NO₂, H₂O, CO...

Temperature: RT – 700°C

Pressure: 1- 5 bar

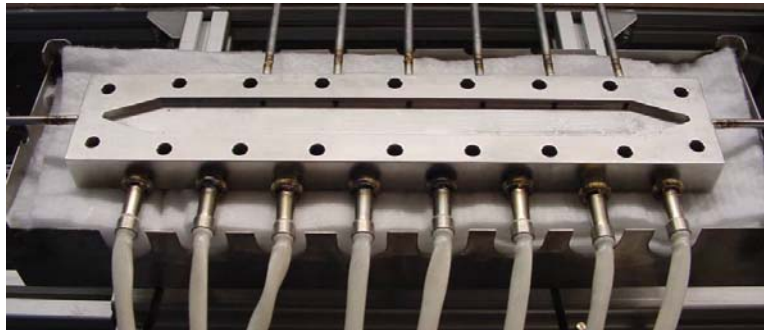
Flow: 10 - 70 slpm

Gas analytics: FTIR, (MS)



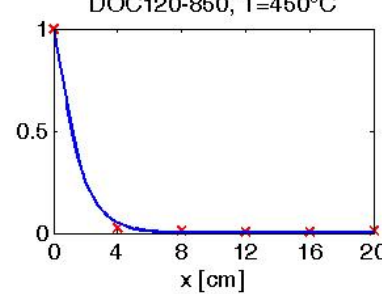
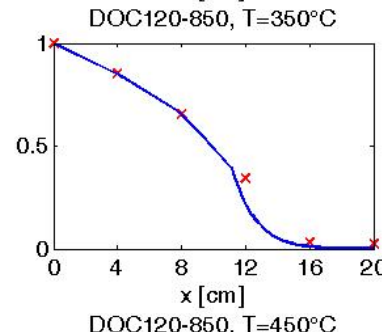
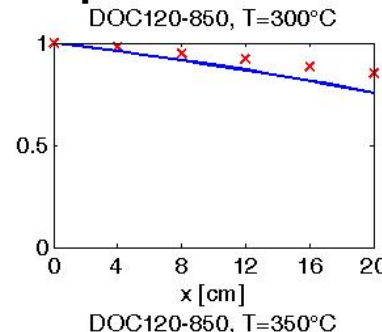
www.abgaszentrum-karlsruhe.de

Isothermal flat bed reactor: Spatially and time-resolved exhaust-gas composition in catalyst channel

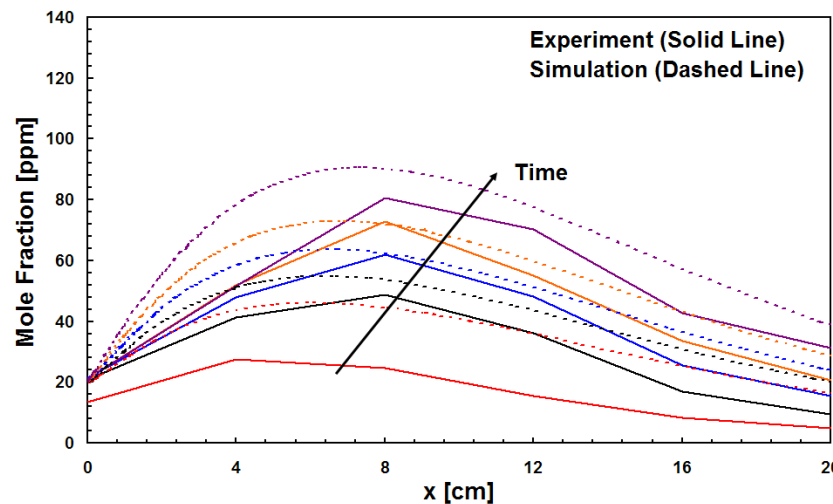


G. Eigenberger et al.

CO profile in DOC



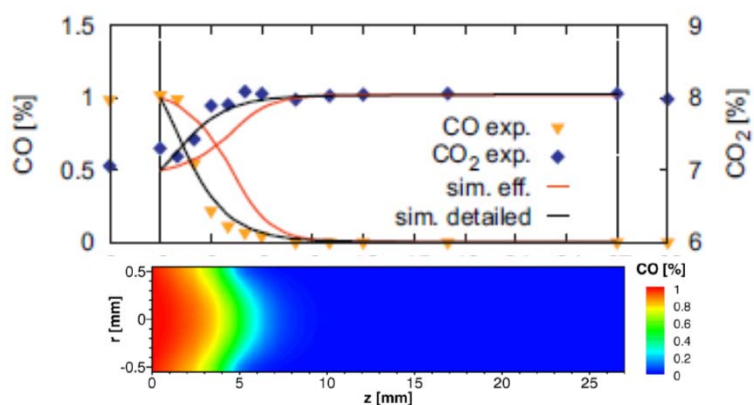
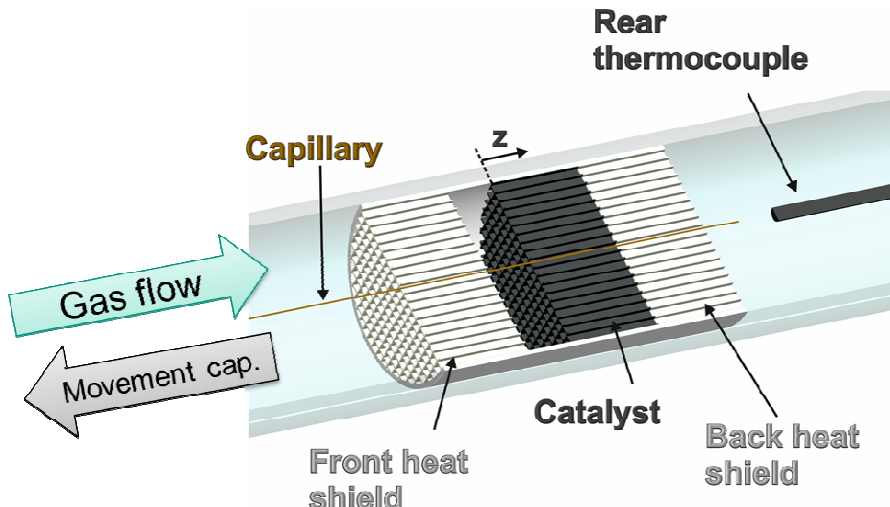
NO₂ profile in NSC during storage



J. Koop, O. Deutschmann. SAE 2007-01-1142.
J. Koop, O. Deutschmann. Appl. Catal.B: Env. 91 (2009) 47

V. Schmeißer, J. Perez, U. Tuttles, G. Eigenberger, Top. Catal. 42 (2007) 15

Lab test bench SpaciPro: Invasive in-situ technique for axially resolved profiles



D. Chan, S. Tischer, J. Heck, C. Diehm, O. Deutschmann.
Applied Catalysis B: Environmental 156–157 (2014) 153.

Tests of catalytically coated honeycombs ($d = 2 - 2.54$ cm,
length ~ 5 cm)

Axially resolved profiles of species concentration, gas-phase and surface temperatures (resolution: 0.25 mm)

Gases: Gaseous and liquid HCs, CO,
CO₂, NH₃, NO, NO₂, O₂,
Air, N₂, H₂, H₂O

Temperature: RT – 1000°C

Pressure: 1 atm

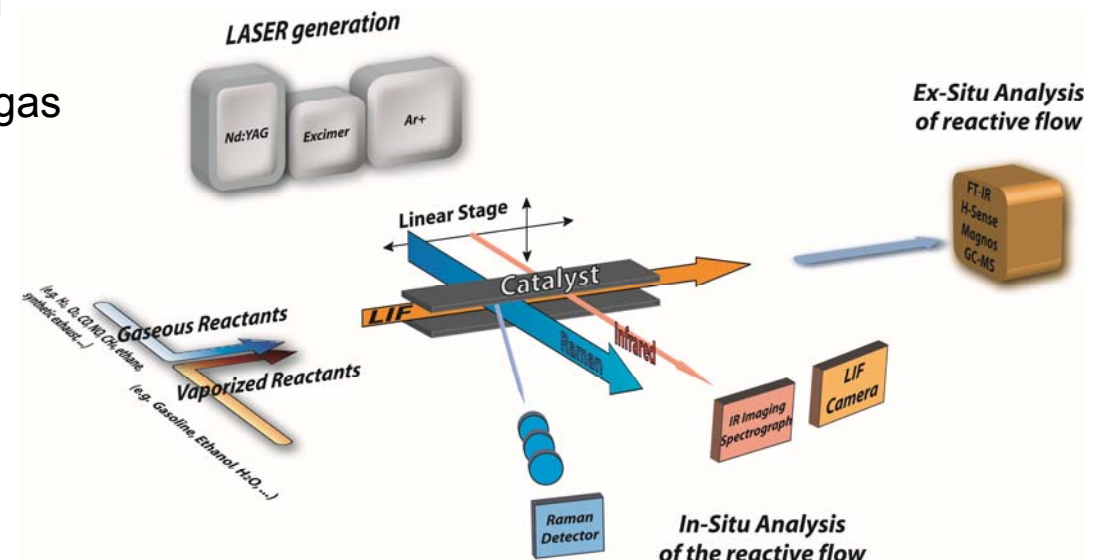
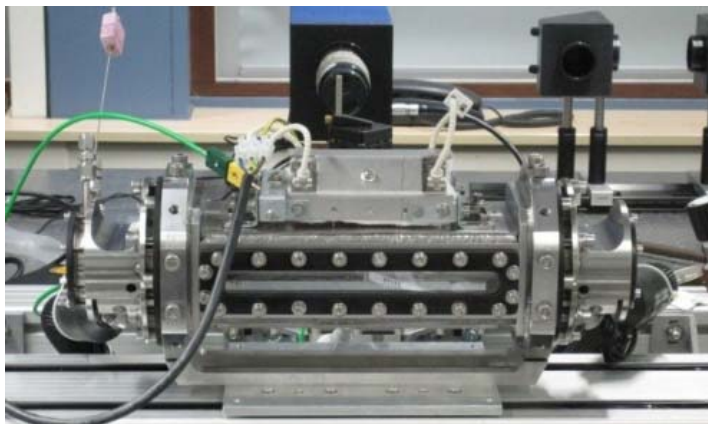
Flow: 0.5 - 5 slpm

Gas analytics: FT- IR, MS, GC

- G. Fisher et al., 2006
R. Horn, N. J. Degenstein, K. A. Williams, L. D. Schmidt, *Catal. Lett.* 110 (2006) 169.
J. Sá, D.L. Abreu Fernandes, F. Aiouache, A. Goguet, C. Hardacre, D. Lundie, W. Naeem,
W.P. Partridge, C. Stere, *Analyst* 135 (2010) 2260.
A. Donazzi, D. Livio, M. Maestri, A. Beretta, G. Groppi, E. Tronconi, P. Forzatti, *Angew. Chem. Int. Ed.* 50 (2011) 3943.
D. Livio, C. Diehm, A. Donazzi, A. Beretta, G. Groppi, O. Deutschmann, *Appl. Catal. A* 467 (2013) 530.

Lab test bench CATHLEN: Optical diagnostics of catalytic reactors

Non-invasive in-situ analysis of spatial and temporal profiles of species concentration and temperature in the gas phase above a catalytic surface using Raman and LIF-spectroscopy

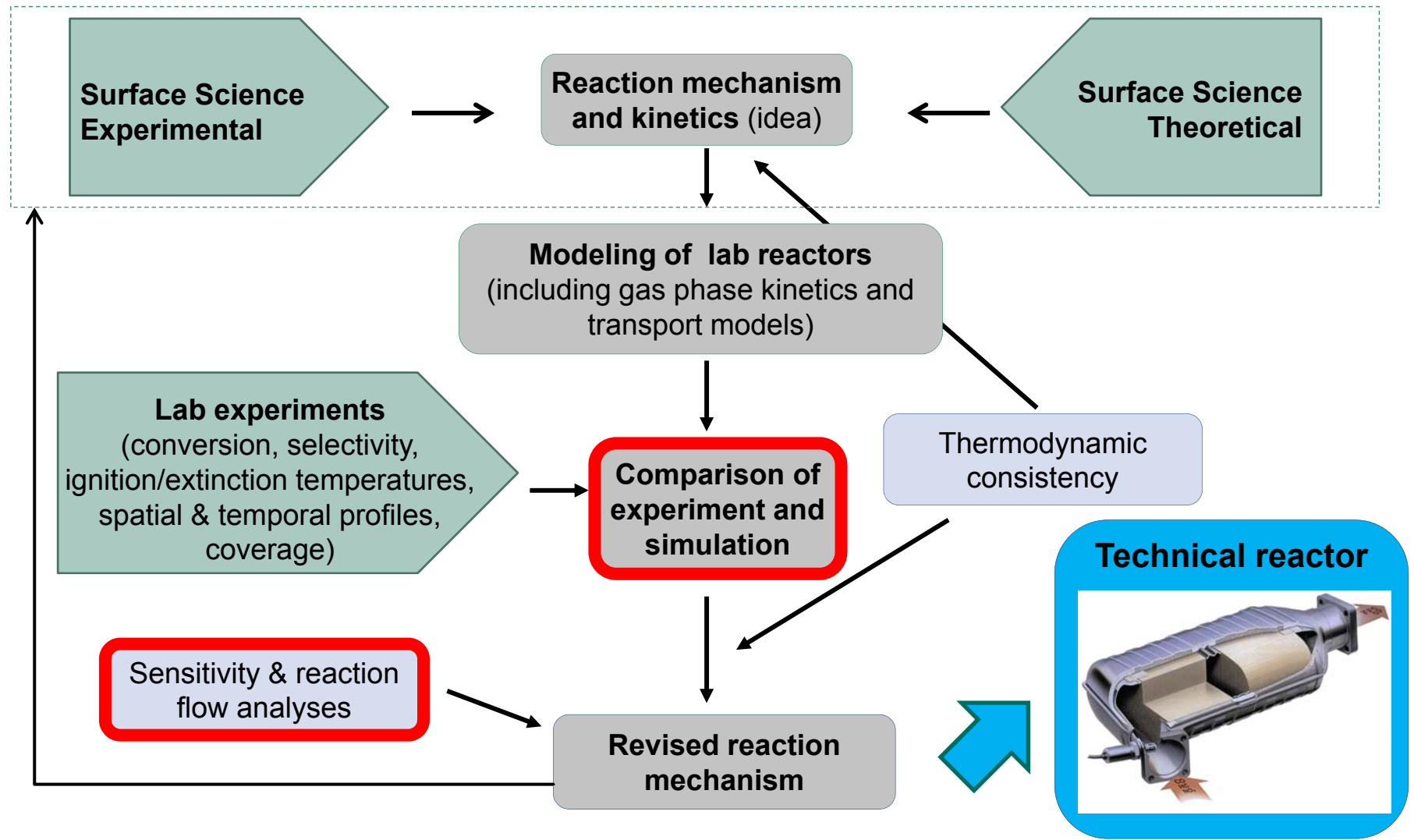


NO LIF profile during reduction by H₂ to NH₃ in Pt/Al₂O₃ one-side-coated single channel of a DOC



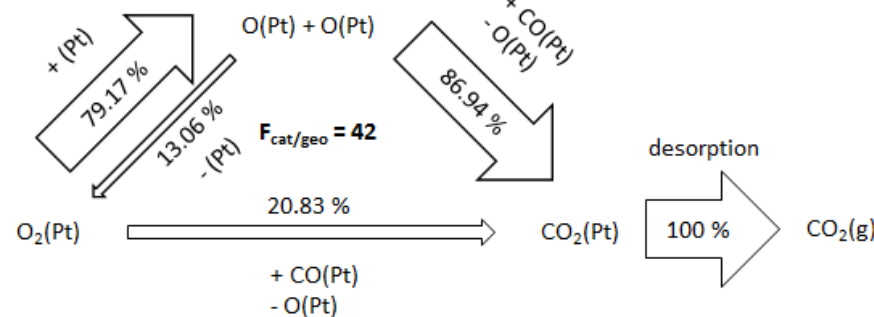
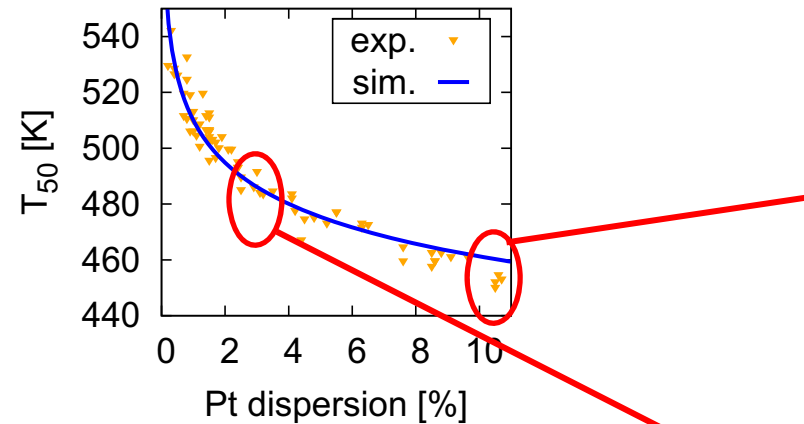
A. Zellner, R. Suntz, O. Deutschmann, Angew. Chem. Intl. Ed. 54 (2015) 2653.

Development of micro kinetic models for simulations of catalytic reactors

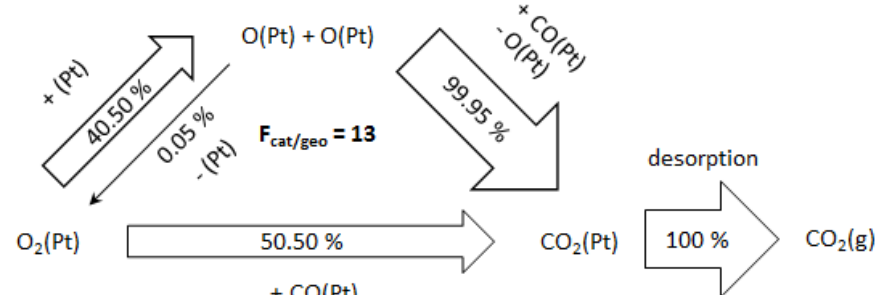


Effect of catalyst loading on conversion of CO in DOC

Reaction flow analysis

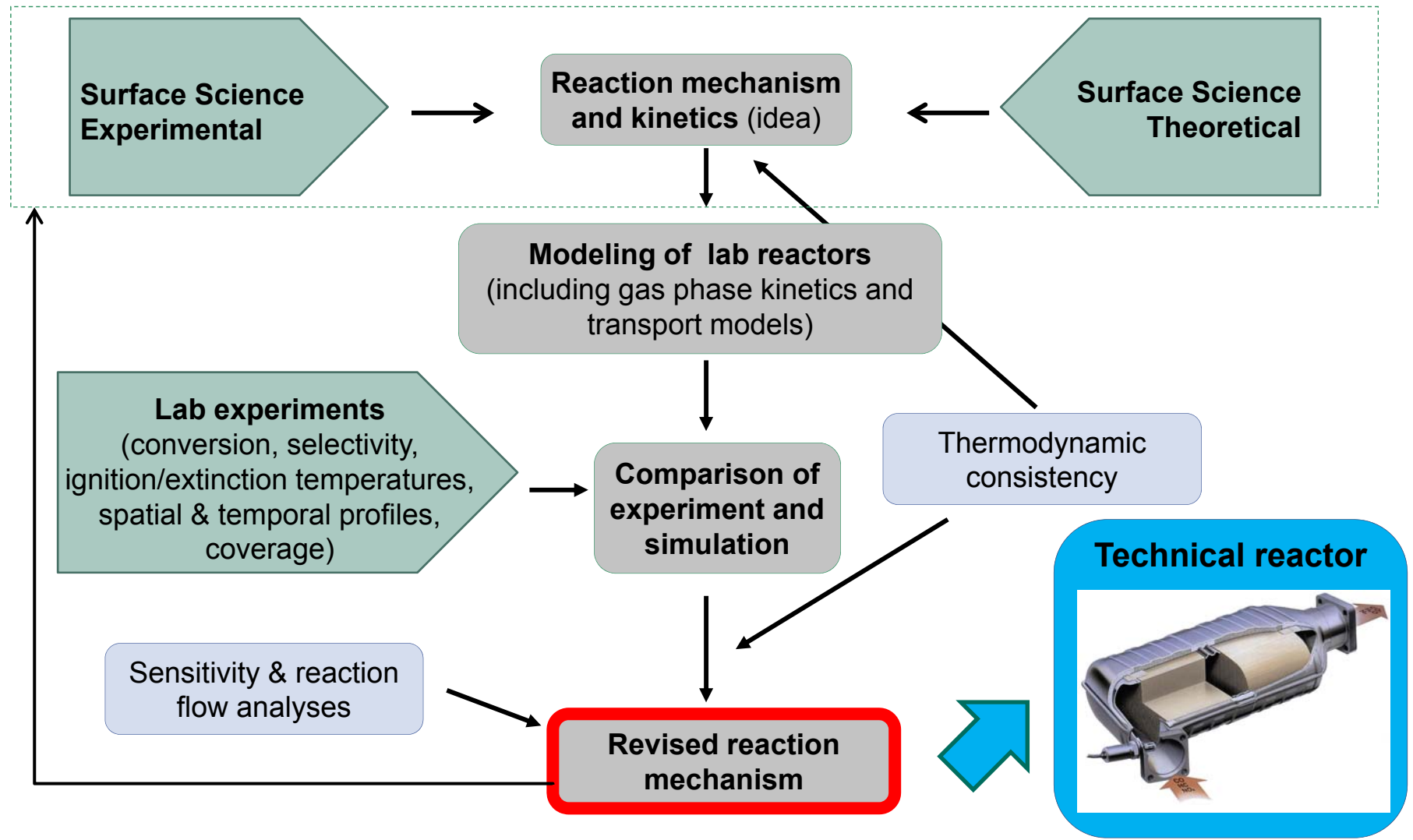


Reaction		A [mol, cm, s] / S^0	β	E_a [kJ/mol]
$O_2 + (Pt)$	\rightarrow	$O_2(Pt)$	5.000 $\times 10^{-2}$	0.000
$O_2(Pt)$	\rightarrow	$O_2 + (Pt)$	5.243 $\times 10^{11}$	-0.069
$O_2(Pt) + (Pt)$	\rightarrow	$O(Pt) + O(Pt)$	8.325 $\times 10^{18}$	0.000
$O(Pt) + O(Pt)$	\rightarrow	$O_2(Pt) + (Pt)$	4.444 $\times 10^{21}$	264.067
				$-88.2 \times \Theta_O$
$CO + (Pt)$	\rightarrow	$CO(Pt)$	8.400 $\times 10^{-1}$	0.000
$CO(Pt)$	\rightarrow	$CO + (Pt)$	7.635 $\times 10^{12}$	-0.139
				$-29.3 \times \Theta_{CO}$
$CO_2 + (Pt)$	\rightarrow	$CO_2(Pt)$	3.193 $\times 10^{-3}$	-0.035
$CO_2(Pt)$	\rightarrow	$CO_2 + (Pt)$	1.894 $\times 10^{10}$	0.139
$CO(Pt) + O_2(Pt)$	\rightarrow	$CO_2(Pt) + O(Pt)$	4.124 $\times 10^{18}$	0.069
				$+44.1 \times \Theta_O$
$CO_2(Pt) + O(Pt)$	\rightarrow	$CO(Pt) + O_2(Pt)$	2.910 $\times 10^{23}$	-0.069
				$+29.3 \times \Theta_{CO}$
$CO(Pt) + O(Pt)$	\rightarrow	$CO_2(Pt) + (Pt)$	4.764 $\times 10^{18}$	0.069
				$-29.3 \times \Theta_{CO}$
$CO_2(Pt) + (Pt)$	\rightarrow	$CO(Pt) + O(Pt)$	6.297 $\times 10^{20}$	-0.069
				$+44.1 \times \Theta_O$

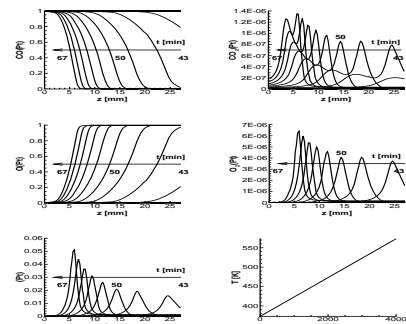
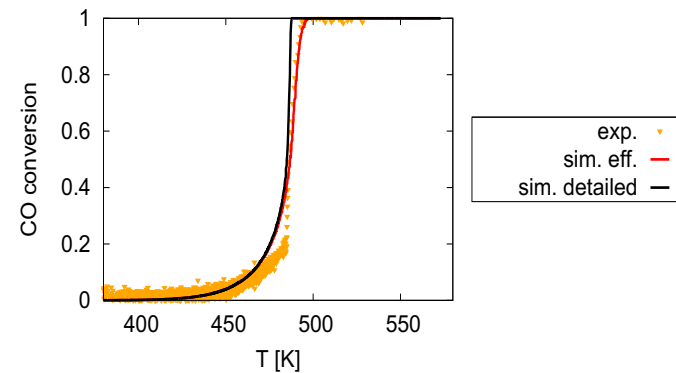
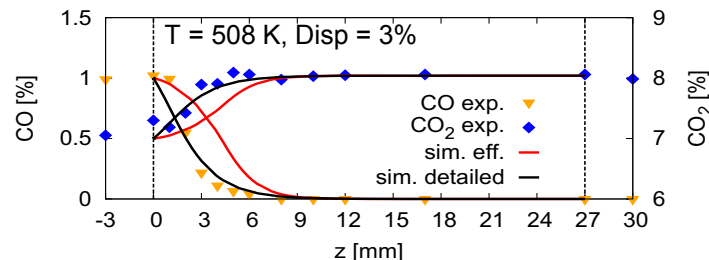


D. Chan, S. Tischer, J. Heck, C. Diehm, O. Deutschmann. Applied Catalysis B: Environmental 156–157 (2014) 153.

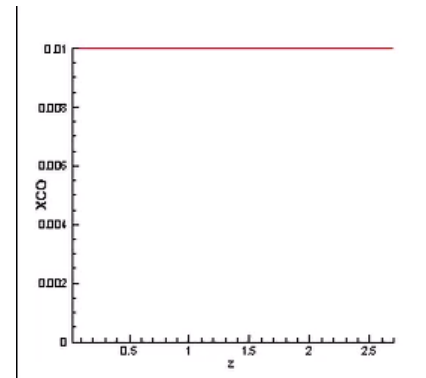
Development of micro kinetic models for simulations of catalytic reactors



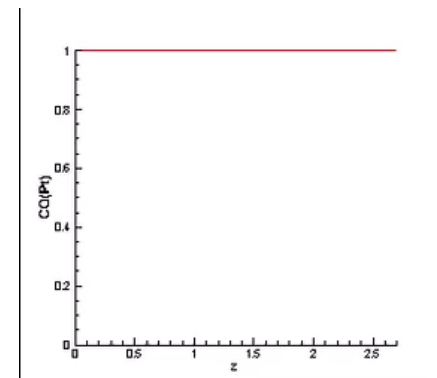
Transient simulation of lab light-off experiment: Temporal variation of axial profiles during light-off



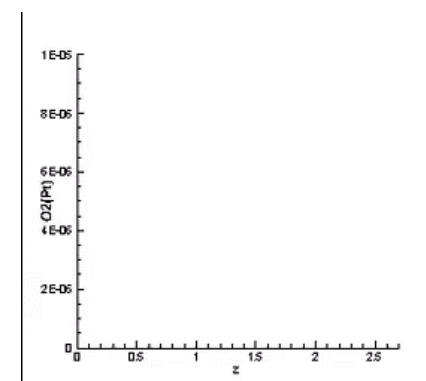
CO



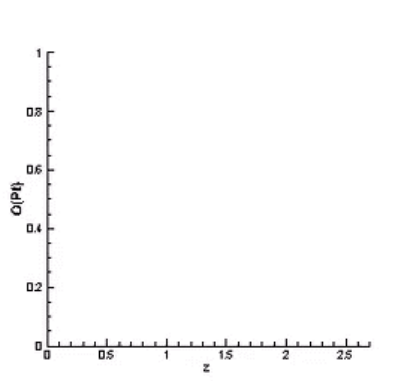
CO(Pt)



O₂(Pt)

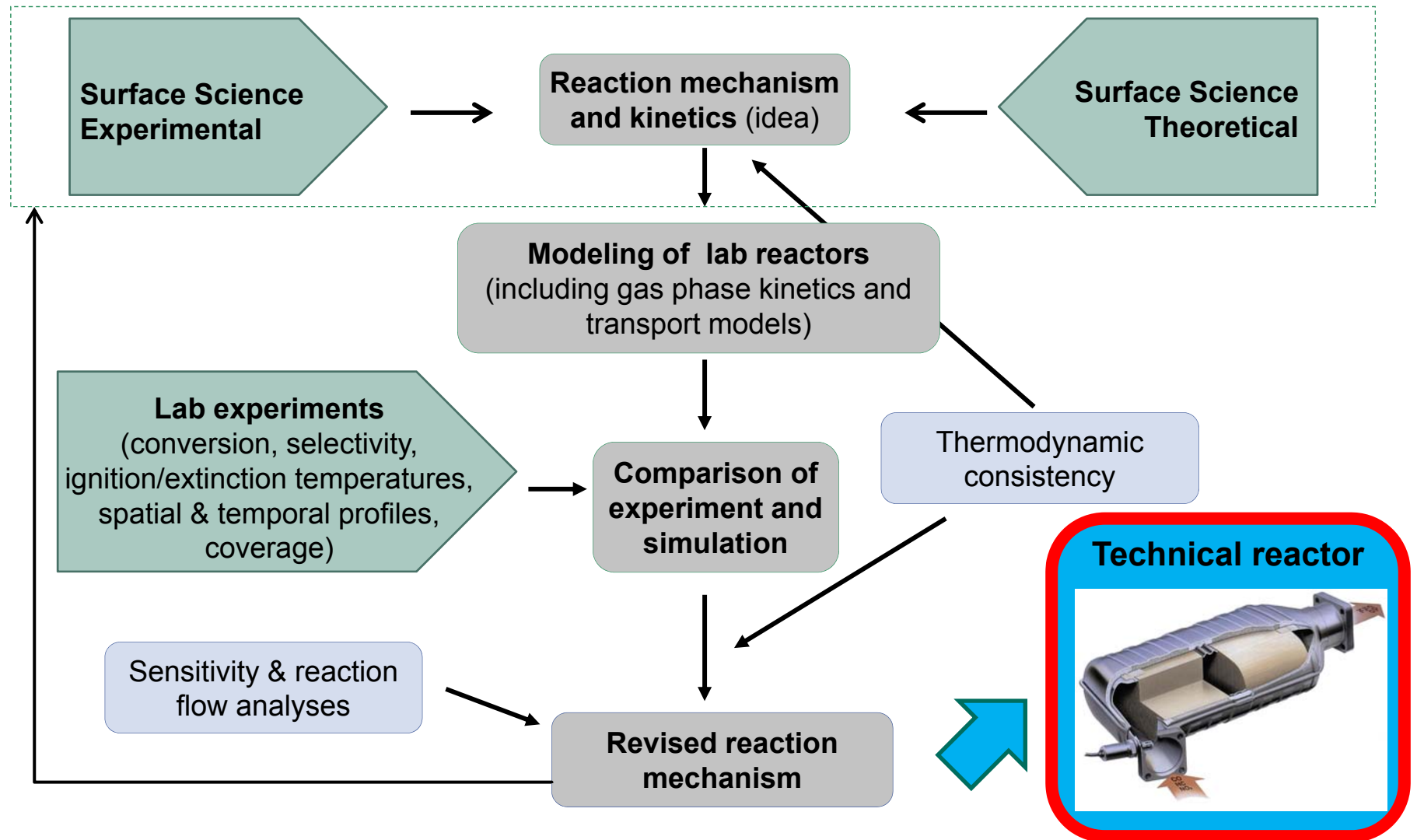


O (Pt)

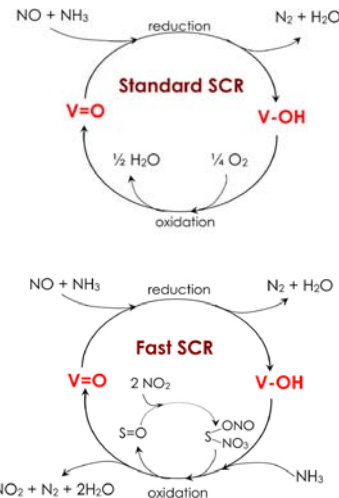
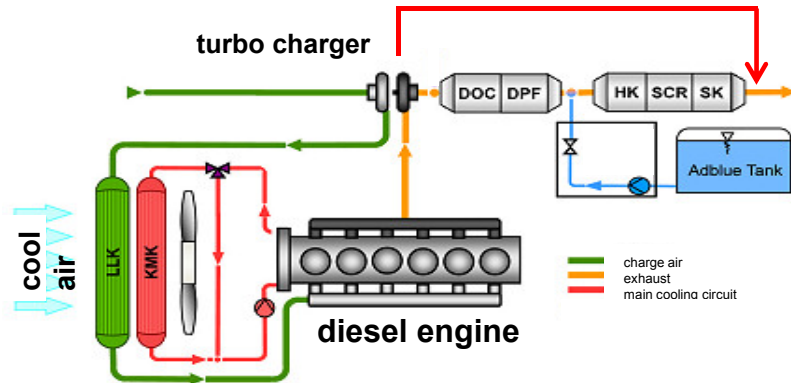


D. Chan, S. Tischer, J. Heck, C. Diehm, O. Deutschmann. Applied Catalysis B: Environmental 156–157 (2014) 153.

Development of micro kinetic models for simulations of catalytic reactors



Pre-turbo SCR for large diesel engines: Effect of high pressure and temperature on conversion

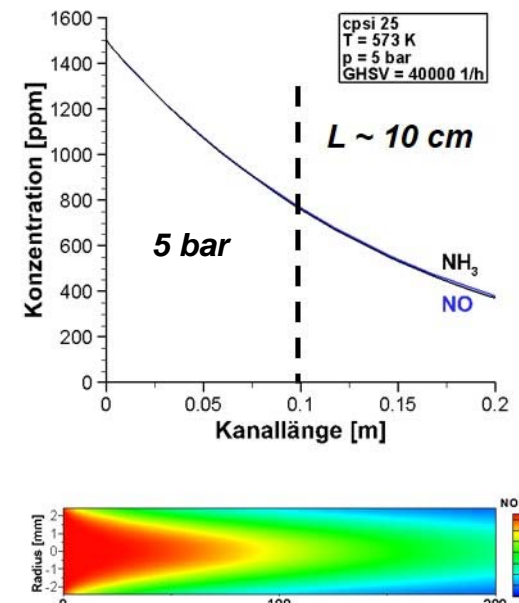
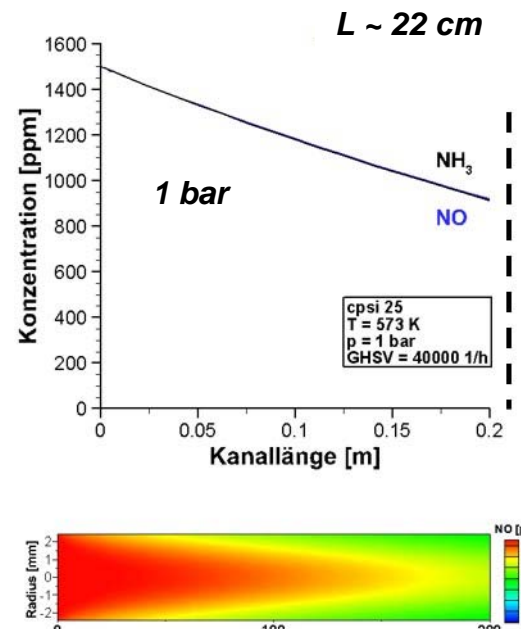


E. Tronconi, I. Nova, C. Ciardelli, D. Chatterjee, M. Weibel; J. Catal. 245 (2007) 1.

I. Nova, C. Ciardelli, E. Tronconi, D. Chatterjee, M. Weibel; (2009), AIChE J.55, 6, 1514-1529

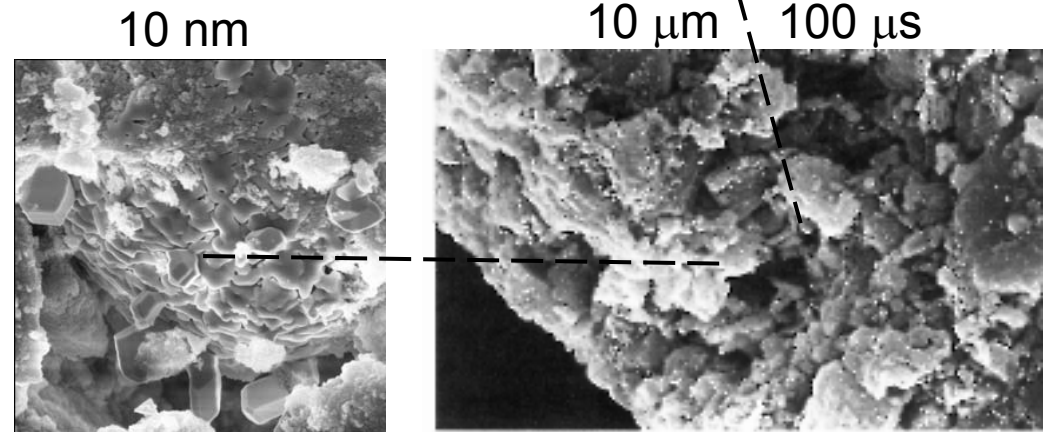
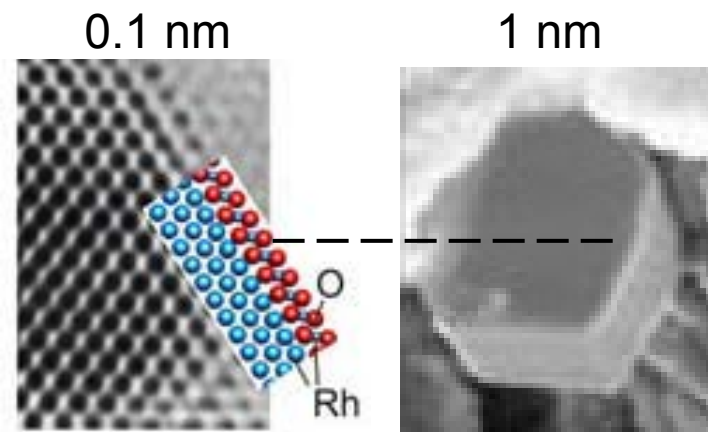
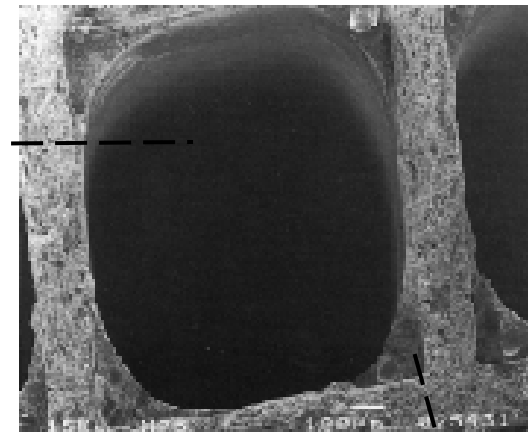
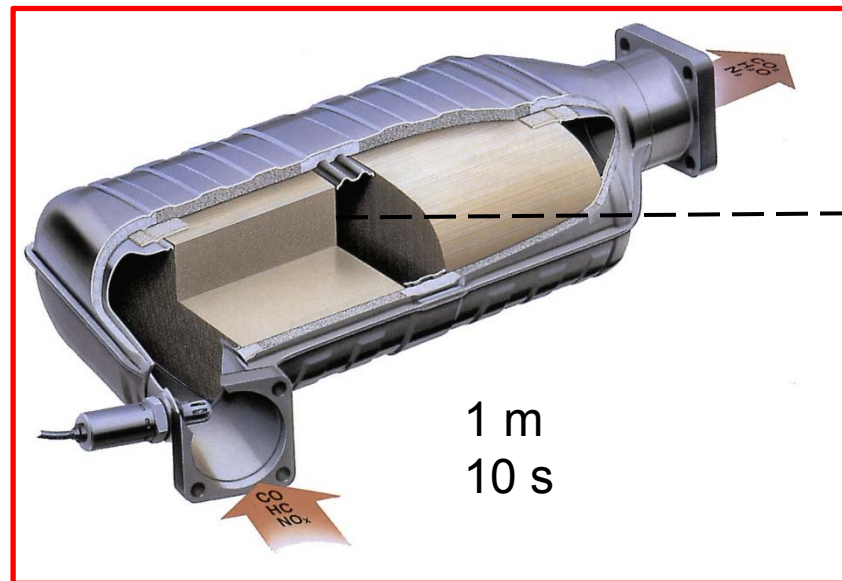
At constant mass flow:

Residence time \sim pressure
Diffusion $\sim 1/\text{pressure}$

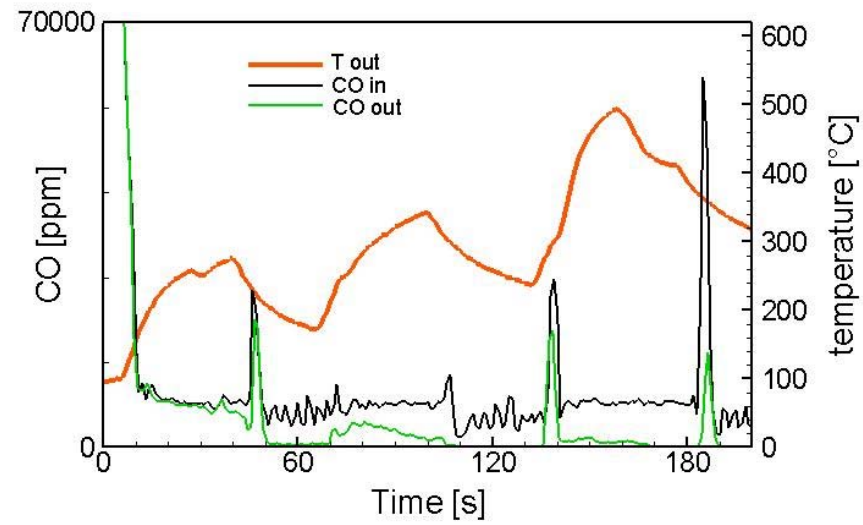
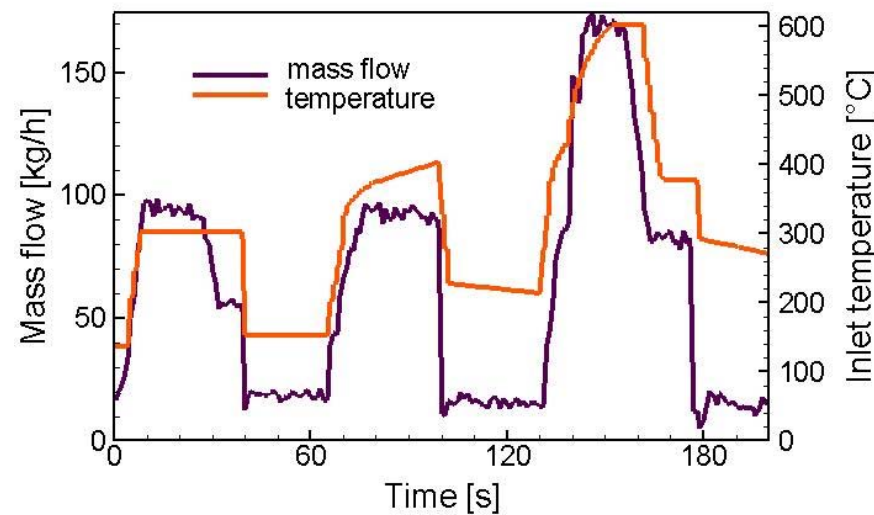


C. Hauck, O. Deutschmann, 2014

Multi-scale modeling: From 10^{-10} m and 10^{-13} s to 1m and 10 s

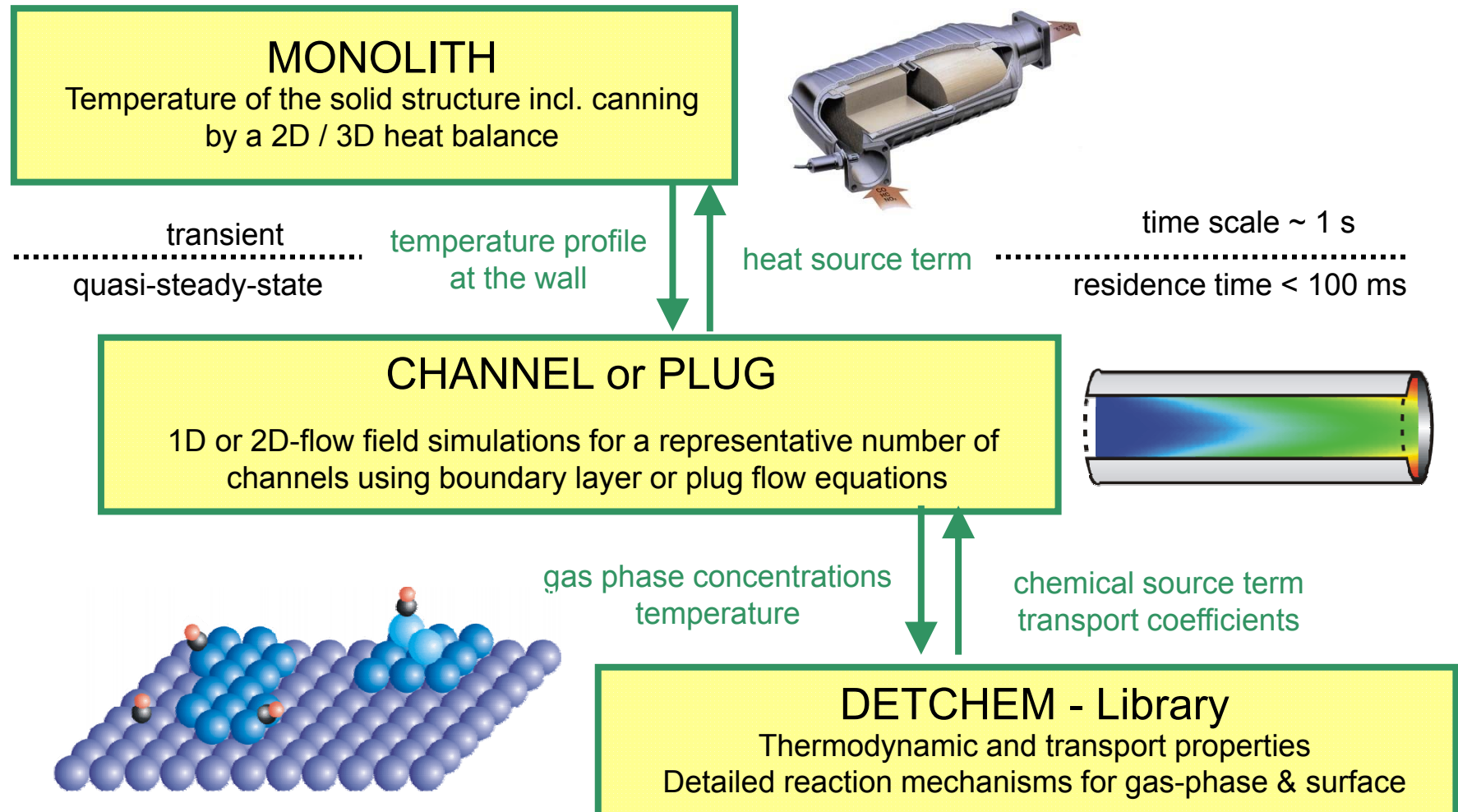


Simulation at real driving conditions is very challenging: Continuous variation of all inlet variables



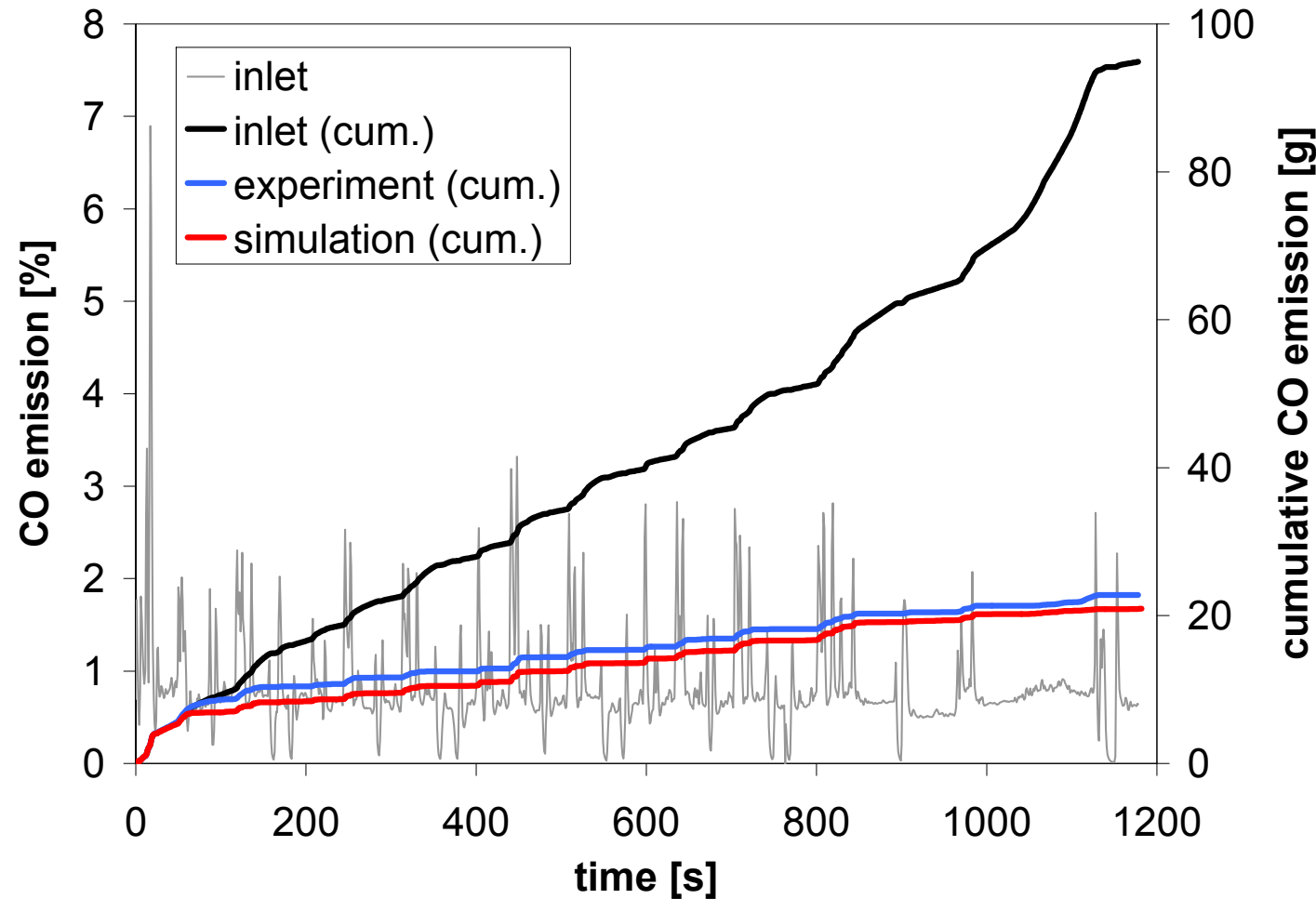
J. Braun, T. Hauber, H. Többen, J. Windmann, P. Zacke, D. Chatterjee, C. Correa, O. Deutschmann, L. Maier, S. Tischer, J. Warnatz, SAE paper 2002-01-0065

DETACHEM^{MONOLITH}: Computer program for the numerical simulation of transients in catalytic monoliths



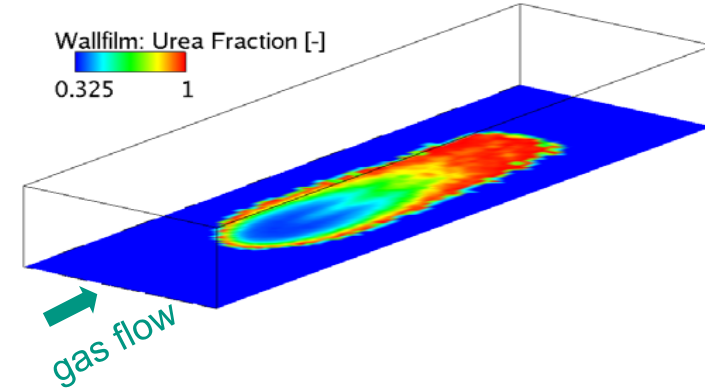
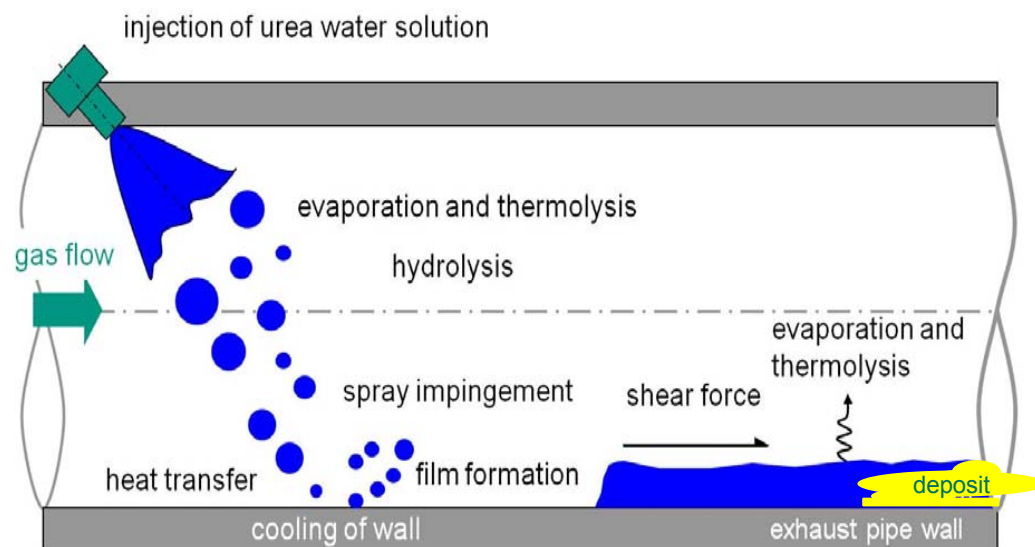
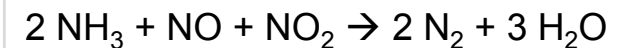
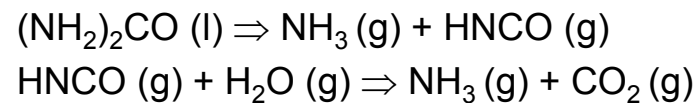
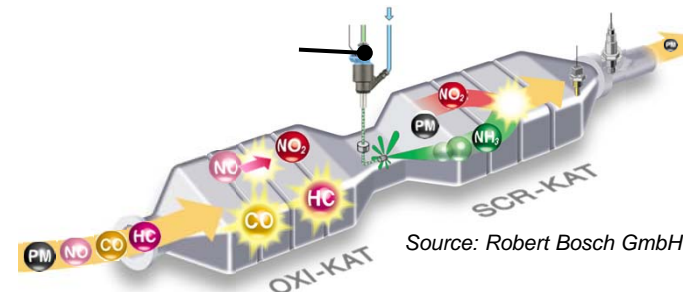
S. Tischer, O. Deutschmann, Catal. Today 105 (2005) 407, www.detchem.de

Cumulative CO emission in MEVG cycle: Experiment vs. simulation



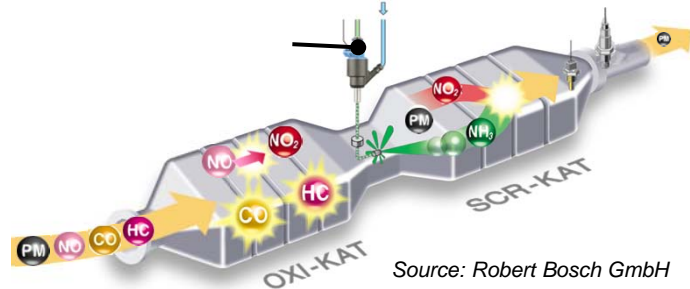
Tischer et al. SAE Technical paper 2007-01-1072 2007

Selective catalytic reduction (SCR) of NO_x emissions by urea solution: Processes between injection and catalyst

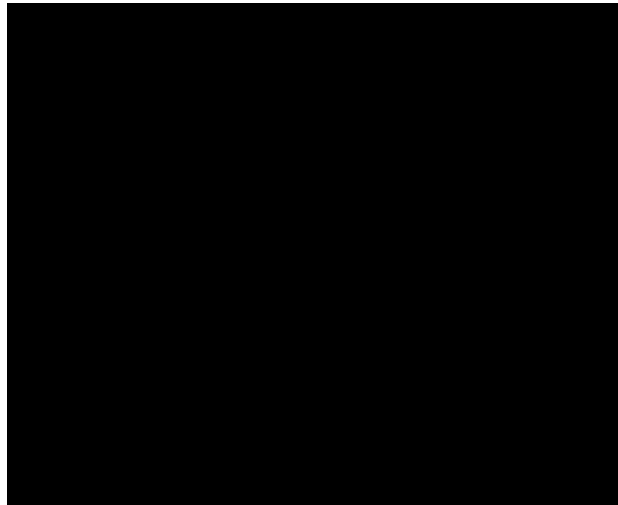


F. Birkhold, U. Meingast, P. Wassermann, O. Deutschmann. SAE Technical paper 2006-01-0643, SAE 2006 Trans. J. of Fuels and Lubricants (2006), 252
F. Birkhold, U. Meingast, P. Wassermann, O. Deutschmann. Appl. Catal. B: Environmental 70 (2007) 119-127

Modeling of deposit formation in Urea-SCR: Understanding the reaction mechanism



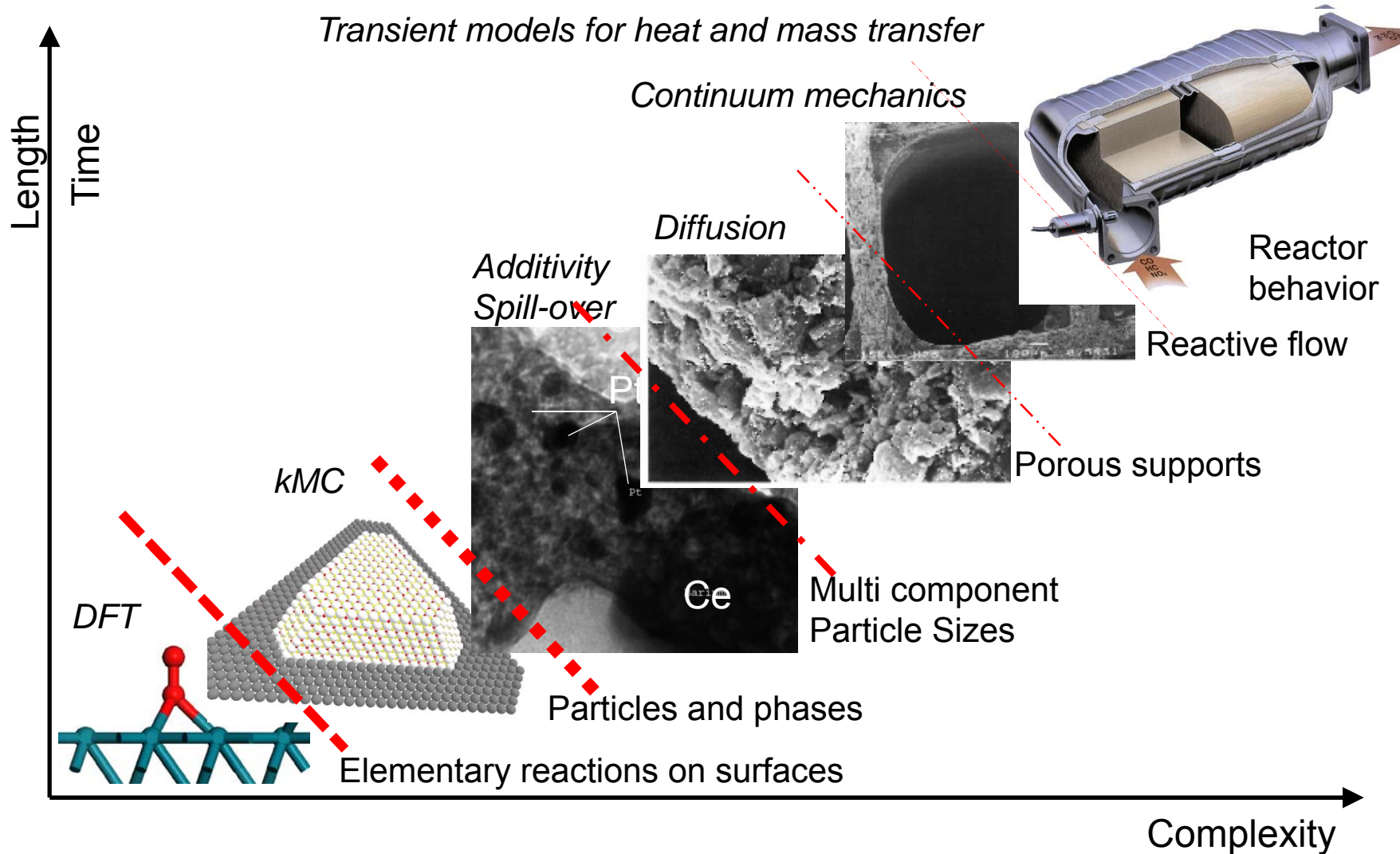
Source: Robert Bosch GmbH



Reaction	γ_j	A	E_A (kJ/mol)
I $CY_{(s)} \rightarrow 3HNCO_{(g)}$	0	1.001×10^3 mol/s	118.42
II $biuret_{(m)} \rightarrow urea_{(m)} + HNCO_{(l)}$	1	1.107×10^{20} 1/s	208.23
III $urea_{(m)} + HNCO_{(l)} \rightarrow biuret_{(m)}$	1 / 1	3.517×10^{11} ml/mol s	75.45
IV $urea_{(m)} \rightarrow HNCO_{(l)} + NH_3_{(g)}$	0.3	2.000×10^4 mol ^{0.7} /ml ^{0.7} s	74.00
V $2biuret_{(m)} \rightarrow ammelide_{(s)} + HNCO_{(l)} + NH_3_{(g)} + H_2O_{(g)}$	2	3.637×10^{26} 1/s	257.76
VI $biuret_{(m)} + HNCO_{(g)} \rightarrow CY_{(s)} + NH_3_{(g)}$	1 / 1	9.397×10^{20} ml/mol s	158.68
VII $biuret_{(m)} + HNCO_{(g)} \rightarrow triuret_{(s)}$	1 / 1	1.091×10^{15} ml/mol s	116.97
VIII $triuret_{(s)} \rightarrow CY_{(s)} + NH_3_{(g)}$	1	1.238×10^{18} 1/s	194.94
IX $urea_{(m)} + 2HNCO_{(l)} \rightarrow ammelide_{(s)} + H_2O_{(g)}$	1 / 2	1.274×10^{20} ml ² /mol ² s ²	110.40
X $biuret_{(m)} \rightarrow biuret_{(matrix)}$	1	8.193×10^{26} 1/s	271.50
XI $biuret_{(matrix)} \rightarrow biuret_{(m)}$	1	3.162×10^{09} 1/s	122.00
XII $biuret_{(matrix)} \rightarrow 2HNCO_{(g)} + NH_3_{(g)}$	1	5.626×10^{24} 1/s	266.38
XIII $urea_{(s)} \rightarrow urea_{(m)}$	1	$1.000 \times 10^{15} \cdot T^{1.5}$ 1/s	160.00
XIV $ammelide_{(s)} \rightarrow ammelide_{(g)}$	1	1.000×10^{14} ml/mol s	201.67
XV $HNCO_{(l)} \rightarrow HNCO_{(g)}$		Herz-Knudsen-equation (Huthwelker and Peter, 1996)	

W. Brack, B. Heine, F. Birkhold, M. Kruse, G. Schoch, S. Tischer, O. Deutschmann. Chem. Eng. Sci. 106 (2014) 1–8.

Simulation of catalytic converters from first principles: Dream or nightmare?



Acknowledgements - Exhaust-Gas After-Treatment



Deutschmann group at KIT 2011



Dr. Denise Chan



A. Gremminger



Dr. Claudia Diehm



Wolfgang Brack



Dr. Ch. Hauck



Dr. Luba Maier



Dr. Steffen Tischer

Academic collaborations

J.-D. Grunwaldt & many colleagues at KIT

U. Nieken, G. Eigenberger (U Stuttgart)
E. Tronconi (Politecnico Milano)
R. Gläser (U Leipzig)
Ch. Beidel, (TU Darmstadt)
G. Wachtmeister (TU München)

SFB/TRR 150 (TU Darmstadt, KIT)

Funding and industry partners



4th International Symposium on Modeling of Exhaust-Gas After-Treatment

MODEGAT IV



Abstract due May 15

13th–15th September, 2015
Bad Herrenalb/Karlsruhe
Germany

J. Emission Control Sci. & Technol. Paper due Aug 31

Thank you!